Induction of human regulatory innate lymphoid cells from group 2 innate lymphoid cells by retinoic acid

Morita, H ; Kubo, Terufumi ; Ruckert, B ; Ravindran, Avinash ; Soyka, M B ; Rinaldi, A O ; Sugita, Kazunari ; Wawrzyniak, Marcin ; Wawrzyniak, P ; Motomura, Kenichiro ; Tamari, M ; Orimo, K ; Okada, N ; Arae, Ken ; Saito, Kazuki ; Altunbulakli, Can ; Castro-Giner, Francesc ; Tan, Ge ; Neumann, A ; Sudo, Katsuko ; O'Mahony, L ; Honda, K ; Nakae, Susumu ; Saito, H ; Mjösberg, J ; Nilsson, Gunnar ; Matsumoto, Kenji ; Akdis, Mübeccel ; Akdis, Cezmi A

Abstract: BACKGROUND: Group 2 innate lymphoid cells (ILC2s) play critical roles in induction and exacerbation of allergic airway inflammation. Thus, clarification of the mechanisms that underlie the regulation of ILC2 activation has received significant attention. Although ILCs are divided into three major subsets that mirror helper effector T-cell subsets, counterpart subsets of regulatory T (Treg) cells have not been well characterized. OBJECTIVE: We sought to determine the factors that induce regulatory ILCs (ILCregs). METHODS: IL-10+ ILCregs induced from ILC2s by retinoic acid (RA) were analyzed using RNA-sequencing and flow cytometry. ILCregs were evaluated in human nasal tissues from healthy individuals and patients with chronic rhinosinusitis with nasal polyp (CRSwNP), and in lung tissues from house dust mite (HDM)- or saline-treated mice. RESULTS: RA induced IL-10 secretion by human ILC2s, but not type-2 cytokines. IL-10+ ILCregs, converted from ILC2s by RA stimulation, expressed a Treg-like signature with the expression of IL-10, CTLA-4 and CD25, with down regulated effector type 2-related markers such as CRTH-2 and ST2, and suppressed activation of CD4+ T cells and ILC2s. ILCregs were rarely detected in human nasal tissue from healthy individuals or lung tissues from saline-treated mice, but were increased in nasal tissues from patients with CRSwNP and in lung tissues from HDM-treated mice. Enzymes for RA synthesis were up-regulated in airway epithelial cells during type-2 inflammation in vivo and by IL-13 in vitro. CONCLUSION: We have identified a unique immune regulatory and anti-inflammatory pathway by which RA converts ILC2s to ILCregs. Interactions between airway epithelial cells and ILC2s play an important roles in the generation of ILCregs.

DOI: https://doi.org/10.1016/j.jaci.2018.12.1018

group 2 innate lymphoid cells by retinoic acid. Journal of Allergy and Clinical Immunology, 143(6):2190-2201.e9.
DOI: https://doi.org/10.1016/j.jaci.2018.12.1018

Accepted Manuscript

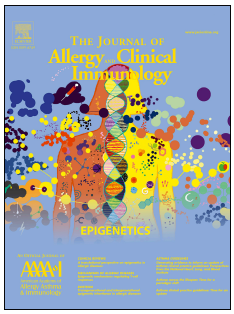

Induction of human regulatory innate lymphoid cells from group 2 innate lymphoid cells by retinoic acid

Hideaki Morita, MD, PhD, Terufumi Kubo, MD, PhD., Beate Rückert, Sci Tec, Avinash Ravindran, Msc, Michael B. Soyka, MD, Arturo Ottavio Rinaldi, Msc, Kazunari Sugita, MD, PhD, Marcin Wawrzyniak, PhD, Paulina Wawrzyniak, PhD, Kenichiro Motomura, MD, PhD, Masato Tamari, MD, PhD, Keisuke Orimo, MD, Naoko Okada, PhD, Ken Arae, PhD, Kyoko Saito, MD, Can Altunbulakli, PhD, Francesc Castro-Giner, PhD, Ge Tan, PhD, Avidan Neumann, PhD, Katsuko Sudo, PhD, Liam O'Mahony, PhD, Kenya Honda, MD, PhD, Susumu Nakae, PhD, Hirohisa Saito, MD, PhD, Jenny Mjösberg, PhD, Gunnar Nilsson, PhD, Kenji Matsumoto, MD, PhD, Mübeccel Akdis, MD, PhD, Cezmi A. Akdis, MD

PII: S0091-6749(19)30088-0

DOI: https://doi.org/10.1016/j.jaci.2018.12.1018

Reference: YMAI 13851

To appear in: *Journal of Allergy and Clinical Immunology*

Received Date: 27 April 2018

Revised Date: 17 December 2018

Accepted Date: 24 December 2018

Please cite this article as: Morita H, Kubo T, Rückert B, Ravindran A, Soyka MB, Rinaldi AO, Sugita K, Wawrzyniak M, Wawrzyniak P, Motomura K, Tamari M, Orimo K, Okada N, Arae K, Saito K, Altunbulakli C, Castro-Giner F, Tan G, Neumann A, Sudo K, O'Mahony L, Honda K, Nakae S, Saito H, Mjösberg J, Nilsson G, Matsumoto K, Akdis M, Akdis CA, Induction of human regulatory innate lymphoid cells from group 2 innate lymphoid cells by retinoic acid, *Journal of Allergy and Clinical Immunology* (2019), doi: https://doi.org/10.1016/j.jaci.2018.12.1018.

Human regulatory innate lymphoid cells are induced from group 2 innate lymphoid cells by retinoic acid

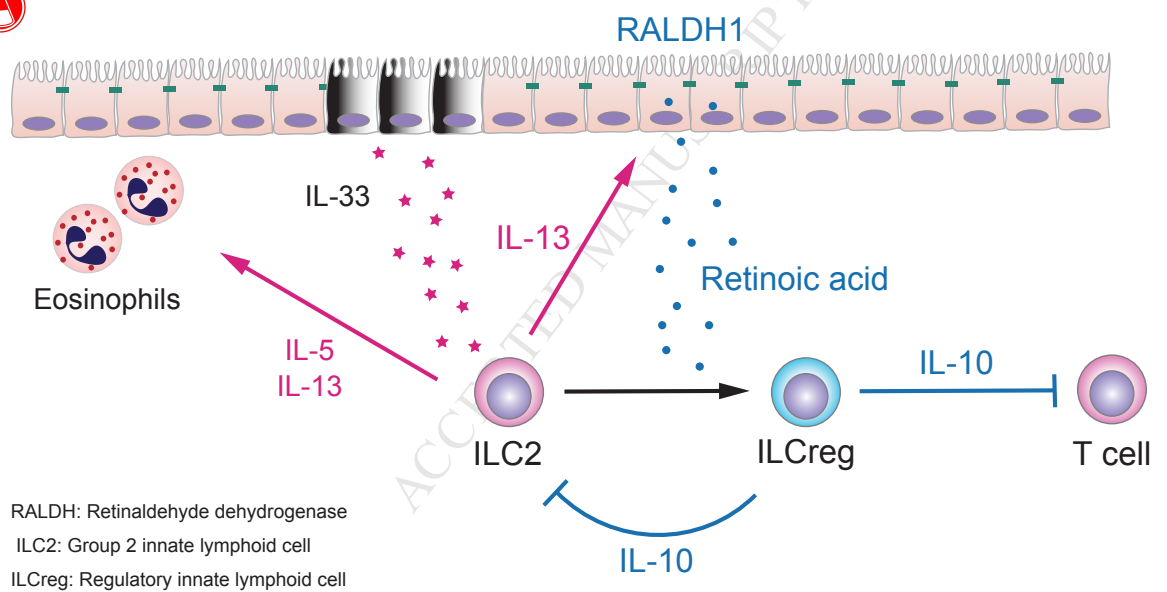

RALDH: Retinaldehyde dehydrogenase

ILC2: Group 2 innate lymphoid cell

ILCreg: Regulatory innate lymphoid cell

Induction of human regulatory innate lymphoid cells from group 2 innate lymphoid cells by retinoic acid

Hideaki Morita MD, PhD,[1,2,3]* Terufumi Kubo MD, PhD.,[1,2] Beate Rückert Sci Tec,[1] Avinash Ravindran Msc,[4] Michael B. Soyka MD,[5] Arturo Ottavio Rinaldi Msc,[1] Kazunari Sugita MD, PhD,[1,2] Marcin Wawrzyniak PhD,[1,2] Paulina Wawrzyniak PhD,[1,2] Kenichiro Motomura MD, PhD,[3] Masato Tamari MD, PhD,[3] Keisuke Orimo MD,[3] Naoko Okada PhD,[3] Ken Arae PhD,[3,6] Kyoko Saito MD,[3] Can Altunbulakli PhD,[1,2] Francesc Castro-Giner PhD,[1,7] Ge Tan PhD,[1,7] Avidan Neumann PhD,[1] Katsuko Sudo PhD,[8] Liam O'Mahony PhD,[1,9] Kenya Honda MD, PhD,[10,11], Susumu Nakae PhD,[12,13], Hirohisa Saito MD, PhD,[3] Jenny Mjösberg PhD,[14] Gunnar Nilsson PhD,[4] Kenji Matsumoto MD, PhD,[3] Mübeccel Akdis MD, PhD,[1,2] Cezmi A. Akdis MD,[1,2]*

1 Swiss Institute of Allergy and Asthma Research (SIAF), University of Zurich, Davos 7270, Switzerland

2 Christine Kühne-Center for Allergy Research and Education, Davos 7265, Switzerland

3 Department of Allergy and Clinical Immunology, National Research Institute for Child Health and Development, Tokyo 157-8535, Japan

4 Immunology and Allergy, Department of Medicine, Karolinska Institutet and Karolinska University Hospital, Stockholm 171 76, Sweden

5 Department of Otorhinolaryngology, Head- and Neck Surgery, University Hospital Zurich and University of Zurich, Zurich 8091, Switzerland

6 Department of Immunology, Faculty of Health Science, Kyorin University, Tokyo 192-8508, Japan

7 Functional Genomics Center Zurich, ETH Zurich/University of Zurich, Zurich 8057, Switzerland

8 Animal Research Center, Tokyo Medical University, Tokyo 160-8402, Japan

9 Department of Medicine and Microbiology, APC Microbiome Ireland, University College Cork, Cork, Ireland

10 Department of Microbiology and Immunology, Keio University School of Medicine, Tokyo 160-8582, Japan

11 RIKEN Center for Integrative Medical Science (IMS), Kanagawa 230-0045, Japan

12 Laboratory of Systems Biology, Center for Experimental Medicine and Systems Biology, The Institute of Medical Science, The University of Tokyo, Tokyo, 108-8639, Japan

13 Precursory Research for Embryonic Science and Technology (PRESTO), Japan Science and Technology Agency, Saitama 332-0012, Japan

14 Center for Infectious Medicine, Department of Medicine, Karolinska University Hospital Huddinge, Karolinska Institutet, Stockholm 171 77, Sweden

*To whom correspondence should be addressed:

Hideaki Morita

2-10-1 Okura, Setagaya-ku, Tokyo 157-8535, Japan

E-mail: morita-hi@ncchd.go.jp

Phone: +81 (3) 3416 0181

and

Cezmi A. Akdis

Obere Strasse 22, CH-7270 Davos Platz, Switzerland

E-mail: akdisac@siaf.uzh.ch

Phone: +41 (0) 81 410 08 48

FAX: +41 (0) 81 410 08 40

Supported by Swiss National Science Foundation grants 310030_156823 and 320030_140772 (to C.A.), Grants-in-Aid for Young Scientists (B) (to H.M.), Banyu Life Science Foundation International (to H.M.), a Grant of National Center for Child Health and Development (#29-2; to H.M.), and Precursory Research for Embryonic Science and Technology, Japan Science and Technology Agency (to S.N.), Heart and Lung Foundation, Swedish Research Council, and The ChAMP (Centre for Allergy Research Highlights Asthma Markers of Phenotype) consortium funded by the Swedish Foundation for Strategic Research, the Karolinska Institutet, and AstraZeneca & Science for Life Laboratory Joint Research Collaboration (to J.M. and G.N.).

Disclosure of potential conflicts of interest: C.A. has consultant arrangements with Actellion, Aventis, Allergopharma and Circacia, and has received grants from Novartis. H.S. has received personal fees from Shiseido Co., Ltd., and AstraZeneca. K. Matsumoto has received speakers' bureaus from MSD (Merck Sharp and Dohme), AstraZeneca, Kyorin Pharmaceutical Co., Ltd., Maruho Co., Ltd and Chugai pharmaceutical Co., Ltd. The rest of the authors declare that they have no conflicts of interest.

Abstract

Background: Group 2 innate lymphoid cells (ILC2s) play critical roles in induction and exacerbation of allergic airway inflammation. Thus, clarification of the mechanisms that underlie the regulation of ILC2 activation has received significant attention. Although ILCs are divided into three major subsets that mirror helper effector T-cell subsets, counterpart subsets of regulatory T (Treg) cells have not been well characterized.

Objective: We sought to determine the factors that induce regulatory ILCs (ILCregs).

Methods: IL-10$^+$ ILCregs induced from ILC2s by retinoic acid (RA) were analyzed using RNA-sequencing and flow cytometry. ILCregs were evaluated in human nasal tissues from healthy individuals and patients with chronic rhinosinusitis with nasal polyp (CRSwNP), and in lung tissues from house dust mite (HDM)- or saline-treated mice.

Results: RA induced IL-10 secretion by human ILC2s, but not type-2 cytokines. IL-10$^+$ ILCregs, converted from ILC2s by RA stimulation, expressed a Treg-like signature with the expression of IL-10, CTLA-4 and CD25, with down regulated effector type 2-related markers such as CRTH-2 and ST2, and suppressed activation of CD4$^+$ T cells and ILC2s. ILCregs were rarely detected in human nasal tissue from healthy individuals or lung tissues from saline-treated mice, but were increased in nasal tissues from patients with CRSwNP and in lung tissues from HDM-treated mice. Enzymes for RA synthesis were up-regulated in airway epithelial cells during type-2 inflammation *in vivo* and by IL-13 *in vitro*.

Conclusion: We have identified a unique immune regulatory and anti-inflammatory pathway by which RA converts ILC2s to ILCregs. Interactions between airway epithelial cells and ILC2s play an important roles in the generation of ILCregs.

Key messages:

・Retinoic acid converts ILC2s into IL-10-producing ILCregs that express CTLA-4.

・ILCregs suppress activation of $CD4^+$ T cells and ILC2s through IL-10 production.

・ILCregs are induced in the airways during type-2 airway inflammation by interacting with epithelial cells to avoid excessive tissue injury and inflammation.

Capsule summary:

This study shows a novel immune regulatory pathway that avoids excessive lung inflammation through conversion of ILC2s to ILCregs by retinoic acid that is synthesized by airway epithelial cells.

Key words: Regulatory innate lymphoid cells, Group 2 innate lymphoid cells, retinoic acid, IL-33, asthma, chronic rhinosinusitis with nasal polyps, CTLA-4 (cytotoxic T-lymphocyte-associated protein 4)

Abbreviation used:

Air-liquid interface: ALI

Bronchoalveolar lavage fluid: BALF

Chemoattractant receptor-homologous molecule on Th2 cells: CRTh2

Chemokine (C-C motif) ligand 5: CCL5

Chronic rhinosinusitis with nasal polyps: CRSwNP

Cytotoxic T-lymphocyte-associated protein 4: CTLA-4

Genome-wide association study: GWAS

Group 1 innate lymphoid cells: ILC1s

Group 2 innate lymphoid cells: ILC2s

Group 3 innate lymphoid cells: ILC3s

House dust mite: HDM

IL-10 receptor: IL-10R

Inducible costimulator: ICOS

Inducible costimulator ligand: ICOSL

Innate lymphoid cells: ILCs

Interferon: IFN

Peripheral Treg cells: pTreg cells

Regulatory T: Treg

Regulatory ILCs (ILCregs)

Retinaldehyde dehydrogenase: RALDH

Retinoic acid: RA

Retinoic acid receptor: RAR

Retinoic acid receptor inhibitor (RAi)

RNA sequencing technologies: RNA-seq

Thymus-derived Treg cells: tTreg cells

Transforming growth factor-β: TGF-β

Introduction

Innate lymphoid cells (ILCs) are newly identified lymphoid lineage immune cells. They do not have rearranged antigen receptors; instead, they respond promptly to multiple cell-derived factors, such as cytokines and eicosanoids, which are released from infected or injured tissues. Like helper T cells, ILCs are currently divided into three distinct subsets according to their transcription factors and signature cytokine production. In brief,

group 1 ILCs (ILC1s) express T-bet and produce interferon (IFN)-γ to control intracellular pathogens such as viruses and intracellular bacteria. Group 2 ILCs (ILC2s) express GATA-3 and produce IL-5 and IL-13 to control helminths. Group 3 ILCs (ILC3s) express ROR-γt and produce IL-17A and IL-22 to control extracellular bacteria.[1-3] Recent reports highlighted the importance of ILCs not only in early immune responses against pathogens, but also in induction and exacerbation of inflammatory diseases.[3-5] ILC2s in particular are known to play crucial roles in allergic diseases such as asthma and chronic rhinosinusitis with nasal polyps (CRSwNP) through production of type-2 cytokines. For instance, a genome-wide association study (GWAS) demonstrated that strong associations between asthma development and genetic polymorphisms in the gene encoding IL-33, which is a major activator of ILC2s,[6] and its receptor IL-1RL1 (ST2).[7] In line with this, the frequency of ILC2s was significantly increased in bronchoalveolar lavage fluid (BALF) from patients with asthma compared to control subjects, and it correlated negatively with airway function,[3] strongly indicating that ILC2s are involved in the pathogenesis of asthma. Numerous studies using various animal models of asthma also elucidated indispensable roles for IL-33 and ILC2s in allergic airway inflammation.[8-12] Moreover, ILC2s were activated as well as increased in nasal tissues from patients with CRSwNP and they were associated with eosinophil infiltration,[13, 14] suggesting that they are involved in allergic diseases induced by type-2 immune responses.

Therefore, regulatory factors that suppress ILC2 activation have received broad attention as new therapeutic targets for allergic diseases. Thus far, our group and others have shown that ILC2 activation was suppressed by regulatory T (Treg) cells through IL-10,[10, 15] transforming growth factor-β (TGF-β),[15, 16] and inducible costimulator (ICOS) and its

ligand inducible costimulator ligand (ICOSL) interaction,[15] as well as recombinant cytokines such as IL-10 and TGF-β.[17] ILC2 activation was also suppressed by type 1 cytokines such as IFN-β,[18, 19] IFN-γ[18–21] and IL-27,[18, 19] and lipid mediators such as prostaglandin I_2 [22] and lipoxin A4.[23]

Very recently, Wang et al. demonstrated the existence of IL-10^+ regulatory ILCs (ILCregs) in mouse and human intestines.[24] They also reported that ILCregs suppressed activation of ILC1s and ILC3s through IL-10 production. However, the existence and roles of ILCregs in the airways remain unclear. In the present study, we demonstrated that a vitamin A metabolite, retinoic acid (RA), induces IL-10-producing ILCregs from ILC2s. *In vitro*, ILCregs induced from ILC2s, acquired a Treg-like signature, down regulate type 2 and an effector lymphocyte signature, and suppressed T cell and ILC2 proliferation through IL-10 production. In addition, we found that ILCregs can be induced from ILC2s in airway tissues during type-2 inflammation in both humans and mice. During type-2 airway inflammation, IL-13, a major type-2 cytokine produced by ILC2s and Th2 cells, induces RA synthesis in airway epithelial cells that may result in induction of ILCregs that control allergic airway inflammation.

Methods

The detailed methods, including experimental protocols and statistical analysis, are presented in the Methods section of this article's Online Repository at www.jacionline.org.

Expansion of human ILC2 lines and clones

Human peripheral blood mononuclear cells (PBMCs) of healthy donors were isolated by gradient centrifugation. After depletion of $CD3^+$, $CD19^+$ and $CD14^+$ cells by AutoMACS (Miltenyi Biotec, Germany), $CD45^+Lin^-CD127^+CRTH2^+CD161^+$ cells were sorted with a FACS Aria II (BD Bioscience, Franklin Lakes, NJ).

$CD45^+Lin^-CD127^+CRTH2^+CD161^+$ cells were expanded in Yssel's medium supplemented with 1% human AB serum, together with irradiated allogeneic PBMCs and 100 U/ml recombinant human IL-2 (Proleukin, Novartis, Basel, Switzerland) for 3 weeks. The typical fold-expansion after 3 weeks was 100 to 500. For human ILC2 clones, after initial sorting of bulk $CD45^+Lin^-CD127^+CRTH2^+CD161^+$ cells with a FACS Aria II as above, the sorted cells were sorted again with FACS Aria II in a single cell mode into a 96-well plates filled with Yssel's medium supplemented with 1% human AB serum, together with irradiated allogeneic PBMCs and 100 U/ml recombinant human IL-2 for 3-week culture.

Flow cytometric analysis

Cell-surface protein and intracellular cytokines and transcription factors were stained by specific antibodies. After staining, the cells were analyzed by ARIA II or LSR Fortessa (BD Bioscience).

Quantitative real-time PCR

Total RNA was extracted and purified using RNeasy Mini Kit and RNeasy Micro Kit (Qiagen, Hilden, Germany) according to the manufacturer's instructions. Total RNA was reverse-transcribed into cDNA using a RevertAid RT kit containing random hexamers (Thermo Fisher Scientific). Quantitative PCR was performed using SYBR green PCR

mix (Thermo Fischer Scientific) on an ABI PRISM 7000 Sequence Detection System (Applied Biosystems, Foster City, CA). Sequences of the primers for detecting target gene expression are listed in Table E2.

RNA isolation and sequencing analysis of RNA-seq data

Total RNA was prepared from sorted $CD45^+Lin^-CD161^+IL\text{-}10^+$ cells and $CD45^+Lin^-CD161^+IL\text{-}10^-$ cells using the RNeasy Plus micro Kit (QIAGEN). Library preparation for RNA-seq was performed using the TruSeq Stranded mRNA Sample Prep Kit (Illumina, CA). Sequencing was performed on an Illumina HiSeq 2500, with paired-end 2x126 bp or single-end 126 bp, using a TruSeq SBS Kit v4-HS (Illumina). Differential expression analysis between two groups was performed using the edgeR Bioconductor package.

Cell isolation from human tissues

Nasal tissues were cut into fine pieces and digested for 45 min at 37°C in RPMI medium (Thermo Fisher Scientific) with 2mg/ml collagenase type II (Worthington, Lakewood, NJ) and 0.04 μg/ml DNase I (Roche, Basel, Switzerland). After incubation, cells were dissociated using GentleMACS Dissociator (Miltenyi Biotec). Lung mononuclear cells were isolated as previously described.[25] In brief, lung tissues were minced and digested for 40 min at 37°C in RPMI medium (Thermo Fisher Scientific) with 0.25 mg/ml collagenase type II (Sigma-Aldrich) and 0.2 mg/ml DNase (Roche). After incubation, the tissues were mechanically disrupted using a 50-ml syringe and 100-μm filter. Cell debris and larger alveolar macrophages were separated by density centrifugation using 30% Percoll (GE Healthcare, Chalfont, UK).

Mice

C57BL/6J wild-type mice were purchased from Japan SLC, Inc. IL-10^{Venus} reporter mice were generated as described previously[26]. All mice were housed under specific-pathogen-free conditions in an environmentally-controlled clean room at the National Research Institute for Child Health and Development (Tokyo, Japan). All experiments were conducted in accordance with the institutional ethical guidelines for animal experiments and safety guidelines for gene manipulation.

Statistical analysis

Statistical analysis of RNA-seq data was performed as described above. Otherwise, all data were analyzed using an unpaired Student's t-test and one-way ANOVA. All analyses were performed using GraphPad Prism (GraphPad Software, La Jolla, CA)

Results

Retinoic acid induces IL-10 production by human ILC2s

Most Treg cells are differentiated in the thymus, and they are termed thymus-derived Treg cells (tTreg cells). However, some Treg cells are generated in the periphery by conversion from $CD4^+Foxp3^-$ T cells, and they are termed peripheral Treg cells (pTreg cells).[27] These facts suggest that Treg cells can be generated in nonlymphoid tissues in response to environmental cues. ILCs are highly plastic,[13, 28-32] thus enabling them to respond promptly to microenvironmental changes. In this context, we hypothesized that ILC2s change their phenotype to a regulatory phenotype in response to certain environmental cues. We first attempted to clarify if factors that contribute to differentiation of pTreg cells, such as TGF-β, RA[33, 34] and vitamin D,[35] convert ILC2

lines into a regulatory phenotype. Among those factors, we found that RA, but neither TGF-β nor vitamin D, induced IL-10 production, which was more pronounced in the presence of IL-33 (Fig 1, A). Next, we investigated whether RA also modulated production of other cytokines/chemokines by ILC2 lines. We observed that RA induced IL-10 production by ILC2 lines in a dose-dependent manner, but it did not enhance production of such type-2 cytokines as IL-5 and IL-13 (Fig 1, B). Conversely, RA suppressed production of an eosinophil-activating chemokine, i.e., chemokine (C-C motif) ligand 5 (CCL5), by ILC2 lines in a dose-dependent manner (Fig 1, B). Since RA was shown to act through its nuclear receptor, retinoic acid receptor (RAR),[36] we included a pan-RAR inhibitor (RAi; BMS 493, Tocris Bioscience, Bristol, UK) to confirm whether these effects were induced through RAR. We found that RAi blocked the effects of RA on ILC2 lines in a dose-dependent manner (Fig 1, C). Taken together, these results demonstrate that RA induces IL-10 production and suppresses CCL5 production by ILC2s through RAR.

IL-10-producing ILCs acquire a Treg cell phenotype

To determine the characteristics of IL-10-producing ILCs induced from ILC2 lines by RA stimulation, we sorted IL-10^+ and IL-10^- ILCs using an IL-10 secretion assay after stimulation with IL-33 and RA (Fig E1, A). Then we performed transcriptome profiling of those cells by high-throughput RNA sequencing technologies (RNA-seq). Hierarchical clustering of the signal intensities of the individual transcripts in each group showed distinct transcript expression patterns for IL-10^+ ILCs and IL-10^- ILCs (Fig E1, B). Of these, IL-10 was the most differentially expressed gene in IL-10^+ ILCs, confirming the quality of our sorting (Table E1). Notably, genes encoding molecules that characterize

ILC2s, such as chemoattractant receptor-homologous molecule on Th2 cells (CRTh2), CD127, OX40 ligand (OX40L) and c-Kit, were distinctly down-regulated in IL-10$^+$ ILCs compared to IL-10$^-$ ILCs (Fig 2, A, B and C) and ILC2 lines (Fig E1, C) at both the transcript and protein levels, suggesting that IL-10$^+$ ILCs induced from ILC2 lines lost their ILC2 signature. However, the expression levels of cytokines and transcription factors for ILC2, such as IL-13 and GATA-3, were not changed in IL-10$^+$ ILCs (Fig 2, C and Fig E1, C). In sharp contrast, genes encoding molecules that characterize Treg cells, such as CTLA-4 and CD25, were distinctly up-regulated in IL-10$^+$ ILCs compared to in IL-10$^-$ ILCs and ILC2 lines (Fig 2, A, D, E, and Fig E1, C), indicating that IL-10$^+$ ILCs induced from ILC2s had acquired a Treg signature. Interestingly, cytokine and transcription factors such as TGF-β, Foxp3, Helios and Aiolos were not changed in IL-10$^+$ ILCs at the protein level (Fig 2, E and Fig E1, C), whereas both IKZF2 and IKZF3, encoding Helios and Aiolos, were significantly upregulated at the transcript level. (Fig 2, A and D). Together these data suggest that IL-10$^+$ ILCs lose the ILC2 phenotype, but acquire a Treg cell phenotype.

ILCregs suppress the proliferation of CD4$^+$T cells and ILC2s through IL-10 production

To confirm the suppressive capacity of IL-10-producing ILCs induced from ILC2 lines by RA, we purified *in vitro*-induced IL-10$^+$ ILCs and IL-10$^-$ ILCs using the IL-10 secretion assay and then co-cultured them with autologous CD4$^+$ T cells or ILC2 lines at different ratios. We found that IL-10$^+$ ILCs suppressed the proliferation of CD4$^+$ T cells induced by anti-CD3 stimulation in a dose-dependent manner (Fig 3, A), whereas IL-10$^-$ ILCs did not (Fig E2, A). This suppressive effect of IL-10$^+$ ILCs was reversed by

312 blocking the IL-10 receptor (IL-10R) (Fig 3, B), but not by blocking CTLA-4 (Fig 3, C),
313 suggesting that IL-10^+ ILCs suppress proliferation of $CD4^+$ T cells through IL-10
314 production. In addition, IL-10^+ ILCs, but not IL-10^- ILCs, showed a dose-dependent
315 suppression of ILC2-line proliferation induced by IL-2 (Fig 3, D and Fig E2, B), which
316 was reversed by blocking IL-10R (Fig 3, E). To compare the suppressive capacity of
317 IL-10^+ ILCs with Treg cells, we purified $CD4^+CD25^{high}CD127^-$Treg cells from peripheral
318 blood and co-cultured them with autologous ILC2 lines at different ratios. We found that
319 the suppressive effect of IL-10^+ ILCs on the proliferation of ILC2 lines was comparable
320 to that of Treg cells (Fig 3, A and Fig E2, C). Taken together, these data clearly show that
321 IL-10^+ ILCs, differentiated from ILC2s, have suppressive function.
322
323 **Human ILC2 clones that are prone to be regulatory ILCs**
324 Next, we sought to determine the stability of IL-10^+ ILCs induced from ILC2. We sorted
325 IL-10^+ and IL-10^- ILCs induced from human ILC2 lines, and then maintained them in a
326 neutral condition, i.e., exposed only to IL-2, for 3 days to allow the cells to rest.
327 Thereafter, half of the cells were stimulated with PMA, ionomycin and monensin, and
328 then stained for IL-10. The other half of the cells were re-stimulated with IL-2, IL-33 and
329 RA for 3 days, followed by PMA, ionomycin and monensin, and then stained for
330 intracellular IL-10. We found that approximately 3.7 % of IL-10^+ ILCs were still able to
331 produce IL-10 even after 3 days' rest, whereas only a marginal proportion of IL-10^- ILCs
332 were (Fig E3). In addition, approximately 23 % of IL-10^+ ILCs were able to produce
333 IL-10 with RA stimulation after 3 days' rest, whereas only a marginal proportion of
334 IL-10^-ILCs were (Fig E3). These findings suggest that IL-10^+ ILCs retained the ability to
335 produce IL-10 in response to RA. They also suggest that there may be a subpopulation of

ILC2s that is capable of being converted to IL-10-producing cells. To confirm that, we generated ILC2 clones from peripheral blood of 5 healthy subjects. We isolated 35 clones and the efficiency of cloning ranged from 4% to 7%. Notably, none of these clones was positive for IL-10 without RA stimulation, but 28% of them (10 of 35 clones) became IL-10-positive when stimulated with RA plus IL-33 (Fig E4, A). In line with this, IL-10 was detected in the culture supernatants of these 10 clones (Fig E4, B), whereas IL-10 was not detected in the culture supernatant of any other clones. These findings confirmed that RA induced IL-10 production only in those 10 clones, but not in the remaining 25 clones. To clarify the difference between the clones that remained IL-10 negative and those that started to produce IL-10 in response to RA stimulation, we determined their expression levels of such surface molecules as c-Kit, CD161 and CTLA-4, before RA stimulation. ILC2s in peripheral blood were shown to have 2 different subsets as a function of c-Kit expression[37]. However, there was no difference in c-Kit expression between the IL-10-secreting and non-secreting groups (Fig E4, C). Similarly, the expression levels of CD161 and CTLA-4 as well as cytokine productions (IL-5 and IL-13) were comparable within the two ILC groups (Fig E4, C and D).

Although human ILC2s, defined as Lin^{-} $CD127^{+}$ $CD161^{+}$ $CRTH2^{+}$ cells, have been thought to be relatively homogeneous compared to ILC1s and ILC3s, our present results indicate that ILC2s are heterogeneous and comprise ILCreg precursors as a subgroup.

ILCregs were induced in nasal tissues from patients with CRSwNP following ILC2 interaction with epithelial cells

The finding of *in vitro* conversion of ILC2 to ILCregs raised the question of whether these ILCregs are also present in human tissues in healthy and certain inflammatory

disease states. To answer this question, we tested nasal tissues from healthy individuals and patients with CRSwNP. We found that ILCregs expressing IL-10 (median number: 9; range: 0-17) or CTLA-4 (median number: 2;, range 5-122) were present in nasal tissues from patients with CRSwNP (Fig 4, A, B and C). Interestingly ILCregs were rarely detected in nasal tissues from healthy subjects (Fig 4, A and B). These results show that the number of ILCregs is significantly upregulated in inflamed tissues, but not in non-inflamed tissues, suggesting that conversion to a regulatory phenotype occurs especially during inflammatory responses. Given that ILCregs were converted from ILC2s by RA stimulation *in vitro*, RA might be induced at local tissue sites during inflammation. To clarify whether RA is induced during inflammation, we determined the mRNA expression for *ALDH1A1*, *ALDH1A2* and *ALDH1A3*, genes encoding for retinaldehyde dehydrogenase (RALDH)1, RALDH2 and RALDH3, respectively, in nasal tissues from the healthy subjects and patients with CRSwNP. RALDHs convert retinal to RA and are responsible for high RA concentrations in the tissues. We found that the expression of *ALDH1A1* was significantly increased in nasal tissues from patients with CRSwNP compared to the healthy individuals (Fig 4, D). In contrast, the expression of *ALDH1A2* was significantly decreased in nasal tissues from patients with CRSwNP compared to the healthy individuals, but the expression levels of *ALDH1A2* were approximately 10-fold less than those of *ALDH1A1* (Fig 4, D). Moreover, the expression of RALDH1 protein was increased in nasal epithelial cells from patients with CRSwNP compared to the healthy individuals (Fig 4, E), indicating that epithelial cells synthesize RA during inflammation. Interestingly, although there is a limitation regarding appropriate lineage markers for exclusion of other immune cell subsets, ILCregs were located in the subepithelial area of the nasal tissues from the patients with CRSwNP (Fig

4, C). In addition, we previously showed possible interaction between ILC2 and bronchial epithelial cells,[38] raising the possibility that interaction between epithelial cells and ILC2s may be important for the conversion of ILC2s into ILCregs. To clarify the factors that promote synthesis of RA in airway epithelial cells, we stimulated air-liquid interface (ALI) cultures of primary bronchial epithelial cells from healthy individuals with IL-5, IL-13 and IL-33. We found that IL-13, but not IL-5 or IL-33, induced expression of *ALDH1A1* and *ALDH1A3* in ALI cultures of primary bronchial epithelial cells (Fig 4, F). These findings suggest that IL-13, a major type-2 cytokine produced mainly by ILC2s and Th2 cells, promoted RA synthesis to induce ILCregs, while inducing allergic airway inflammation. We also investigated human lung tissues to clarify the existence of ILCregs. As in the nasal tissues, ILCregs were rarely detected in mononuclear cells from non-inflamed lung tissues. However, the frequency of IL-10$^+$ ILCs was increased when those cells were stimulated with RA. (Fig 4, G).

Taken together, ILCregs are increased in the inflamed human airway, but are rare in the non-inflamed human airway, and interaction between ILC2s and bronchial epithelial cells at local sites of inflammation may be involved in induction of ILCregs.

ILCregs were induced in the lungs, but not in the mesentery, of intranasally HDM-treated mice

The findings in human nasal tissues indicated that ILCregs do not exist in the airways in a steady state, but are further induced during type-2 inflammation. To further evaluate these findings, we induced allergic airway inflammation by intranasal administration of an HDM extract to IL-10-reporter mice[26]. As previously reported,[39, 40] ILC2s as well as eosinophils were increased in BALFs from HDM-treated mice compared to those in

BALFs from saline-treated mice (Fig 5, A). Importantly, $CD45^+Lin^-IL\text{-}10^+$ cells were detected in BALFs and lungs from HDM-treated mice, but were rarely detected in those specimens from saline-treated mice (Fig 5, B). $CD45^+Lin^-IL\text{-}10^+$ cells in BALFs did not express CD4, but expressed such canonical markers as CD127 and CD90 (Fig 5, C), indicating that these cells are ILCs. $CD45^+Lin^-IL\text{-}10^+$ILCs also expressed Sca-1 and KLRG1, which are lung ILC2 markers[41] (Fig 5, C and E). To compare these cells with ILCregs recently found in the intestine, we determined the expression of a unique transcription factor of ILCregs found in the intestine, i.e., inhibitor of DNA binding 3 (Id3), as well as key ILC2s markers such as GATA-3 and ST2. We found that $IL\text{-}10^+$ ILCs in the lung did not express Id3, whereas they expressed GATA-3 and ST2 (Fig 5, D), indicating that $IL\text{-}10^+$ ILCs in the lungs are distinct from ILCregs in the intestine and may be induced from ILC2s. We also determined the frequency of ILCs in the mesentery, which is the site where ILC2s were originally found.[42] We found that the frequency of ILC2s defined as $CD45^+Lin^-CD127^+Sca\text{-}1^+KLRG1^+$ cells in the mesentery was increased in HDM-treated mice compared to saline-treated mice (Fig 5, F). However, $CD45^+Lin^-IL\text{-}10^+$ILCs were not detected in the mesentery from either saline-treated or HDM-treated mice (Fig 5, F), indicating that ILCregs are induced at local sites of inflammation only in response to environmental cues.

To clarify whether RA is induced in the lung during inflammation, we determined the expression of RALDH-1 protein in lungs from HDM-treated and saline-treated mice. As seen in the nasal tissues from patients with CRSwNP, expression of RALDH-1 protein was markedly increased in the bronchial epithelial cells from HDM-treated mice compared to the saline-treated mice (Fig 5, G).

In summary, as seen in the human nasal tissues, ILCregs are present only in inflamed lungs and RA production by epithelial cells may play important roles.

Discussion

This study is the first to show that human ILCregs can be generated from ILC2s by RA and are present in the sinus tissues of patients with CRSwNP, but are rare in non-inflamed sinus tissues. Since ILCs have been considered to be tissue resident cells, with minimal hematogenous recruitment,[18, 43] it was hypothesized that ILCregs can be induced from effector ILC subsets at local sites of inflammation. Indeed, ILCs are recognized as being highly plastic cells that can convert their phenotype according to environmental cues, enabling them to respond promptly to local microenvironmental changes. For instance, trans-differentiation between ILC1s and ILC3s in the intestinal lamina propria,[28, 29] and between ILC1s and ILC2s in the lung[13, 31, 32] has been reported. *In vitro*, ILC3s differentiated into ILC1s in response to IL-12, while ILC1s differentiated into ILC3s in response to IL-1β, IL-23 and RA.[28, 29] Similarly, ILC2s differentiated into ILC1s in response to IL-1β and IL-12, while ILC1s differentiated into ILC2s in response to IL-4.[13, 30-32]

Vitamin A, which is normally obtained through consumption of certain foods, is needed for a variety of biological functions, including vision, embryonic development, brain function and immunity.[44] Of these, vitamin A, through its metabolite RA, has garnered attention for its roles in immune regulation especially of T cells.[44] For instance, RA was shown to be responsible for differentiation of naïve T cells to Treg cells[34, 45] and to also contributes to the stability and function of Treg cells.[46] Those findings suggest that RA might also act on ILCs and induce ILCregs. *RARG*, the gene encoding retinoic acid

455 receptor gamma, was shown to be expressed in all subsets of human ILCs,[37] suggesting
456 that all ILC subsets can be potentially regulated by RA to some extent. Indeed, RA
457 induced expression of gut-homing receptors such as CCR9 and α4β7 on ILC1s and
458 ILC3s that result in migration of those cells to the intestine.[47] RA, in combination with
459 IL-1β and IL-23, also induced development of ILC3s and enhanced their production of
460 IL-22 in mice.[48-51] In contrast to its positive effects on development and function of
461 ILC3s, RA was reported to inhibit development of ILC2s from ILC2 progenitors in
462 mouse bone marrow.[49] However, the effects of RA on proliferation and cytokine
463 production of mature type-2 immune cells are controversial. Spencer et al. showed that
464 RA suppressed proliferation and cytokine production of mouse ILC2s from the small
465 intestinal lamina propria. RA also suppressed IL-7- and SCF-induced IL-13 production
466 by human peripheral blood $Lin^{-}cKit^{+}CD127^{+}$ILCs.[49] In contrast, Trabanelli et al. showed
467 that RA did not alter IL-13 production by human ILC2 lines stimulated with IL-2, IL-33
468 or prostaglandin D2.[52] In agreement with our data, Seehus et al. recently showed that RA
469 induced production of IL-10, but not IL-13 by mouse ILC2s from the lung in response to
470 stimulation with IL-2, IL-7 and IL-33.[53] In addition, proliferation and type-2 cytokine
471 production of human Th2 cells were shown to be enhanced by RA treatment.[54, 55] This
472 variation may be due to differences in the cell types and stimuli used in each study. RA is
473 synthesized by one of three retinaldehyde dehydrogenases, RALDH1, RALDH2 and
474 RALDH3,[44] whose *in vivo* expression are strictly regulated both temporally and spatially,
475 indicating that expression of RALDHs ensures the ability of each specific cell type to
476 synthesize RA. In the present study, expression of RALDH1 was increased in nasal
477 epithelial cells from patients with CRSwNP (Fig 4, E) and in bronchial epithelial cells
478 from HDM-treated mice (Fig 5, G), suggesting that ILCregs are converted from ILC2s

only in inflamed airway tissues during type-2 airway inflammation. Supporting that concept, ILCregs could not be detected in the mesentery from either saline-treated or HDM-treated mice (Fig 5, F). Others showed that expression of RALDH-1 was increased in bronchial epithelial cells in *Aspergillus*-induced allergic airway inflammation, and its expression was enhanced in matrix metalloproteinase 7 (MMP-7)-deficient mice compared to wild-type mice,[56] suggesting that MMP-7 may be involved in regulation of RALDH-1 expression in bronchial epithelial cells. However, it is unclear how the absence of MMP-7 contributed to higher expression of RALDH-1 in those cells. In our study, RALDH1 expression was significantly increased in ALI-cultured primary bronchial epithelial cells by IL-13 stimulation (Fig 4, F). In addition, while there was only limited RALDH-1 expression in the airways of naïve and saline-treated mice, as previously reported,[56] RALDH-1 expression was increased after induction of allergic airway inflammation (Fig 5, G). These findings indicate that IL-13-a major type-2 effector cytokine produced mainly by ILC2s and Th2 cells during allergic airway inflammation-promotes RA synthesis in bronchial epithelial cells, which in turn may contribute to resolution of allergic airway inflammation. These mechanisms may comprise a negative feedback system for maintaining airway homeostasis.

Since there is substantial heterogeneity in ILCs, recent studies attempted to determine the phenotypes and roles of ILCs in human tissues by analyzing single cells using single-cell RNA sequencing and mass cytometry.[37, 57, 58] However, none of those studies detected the IL-10$^+$ regulatory subset in human tissues. Recently, Wang et al. demonstrated the presence of IL-10$^+$ ILCregs in intestinal specimens from both humans and mice in steady state.[24] In addition, IL-10$^+$ ILCregs were induced in the intestine during intestinal inflammation to suppress activation of ILC1s and ILC3s. In contrast to Treg cells,

intestinal ILCregs did not express Foxp3, suggesting that they are distinct from Treg cells. ILCregs in the intestine expressed ILC markers such as CD127 and Sca-1, but lacked ILC1 markers (i.e., NK1.1 and NKp46), ILC2 markers (i.e., ST2 and KLRG1) and ILC3 markers (i.e., NKp46 and RORγt). In addition, ILCregs in the intestine were derived from $\alpha4\beta7^{+}Id2^{high}$ CHILP (common helper-like innate lymphoid cells precursors), but not their downstream precursor $PLZF^{+}$ ILCP (common ILC precursors), and required Id3 for development, which is unlike other ILC subsets, suggesting that ILCregs in the intestine are distinct from the other effector ILC subsets.[24] In contrast to ILCregs in the intestine, IL-10^{+} ILCregs in the airways were rarely detected in the steady state, but were induced during type-2 inflammation, in both humans and mice (Fig 4, B and Fig 5, B). That suggests that ILCregs in the airways might have been converted from other effector ILC subsets at local sites of inflammation or migrated to the lungs from other organs such as the intestine. However, unlike ILCregs in the intestine, ILCregs in lungs from HDM-treated mice expressed KLRG1, GATA-3 and ST2, which are common markers of ILC2s, but did not express Id3 (Fig 5, C and D). In addition, Id3 was not differentially expressed on *in vitro*-induced human IL-10^{+} ILCregs compared to IL-10^{-} ILCs (Fig E1, D). These findings indicate that IL-10^{+} ILCregs in the lungs and *in vitro*-induced human IL-10^{+} ILCregs may be distinct from ILCregs in the intestine.

Recently, Seehus et al. showed IL-10 producing ILCs, named $ILC2_{10}$, in lungs from IL-33-injected mice.[53] In contrast to the human ILCregs shown in the present study, the gene encoding CTLA-4 was not differentially expressed in those $ILC2_{10}$ found in the lungs from IL-33-injected mice. In addition, transcription factors such as Atf3 and Foxf1, previously shown to be highly expressed on $ILC2_{10}$, were not differentially expressed on *in vitro*-induced human IL-10^{+} ILCregs compared to IL-10^{-} ILCs (Fig E1, D). Therefore,

like other subsets of ILCs and Tregs, ILCregs have different phenotypes and roles depending on the type of tissue, inflammation and animal model. Further studies, including single-cell analysis of ILCregs from different types of tissues, are needed to better understand the ILCreg subset. Regarding the stability of ILCregs, since human IL-10-producing ILCregs induced from ILC2s retained their ability to produce IL-10 in response to RA, but not without RA, after 3 days' rest (Fig E3), RA could be of critical importance in maintaining ILCregs' expression of IL-10. Interestingly, IL-10 non-producing ILCs did not produce IL-10 even if the cells were re-stimulated with RA after 3 days' rest (Fig E3), indicating that there may be a subpopulation of ILC2s that is capable of being converted to IL-10^+ ILCregs. In the HDM-induced asthma-like model, IL-10^+ Tregs as well as IL10^+ ILCregs, but less IL-10^+ Bregs, were increased in lungs from HDM-treated mice (Fig E5, A and B). It is assumed that ILCregs may have suppressive capacity *in vivo* and have different roles compared to Treg and Breg cells in terms of antigen specificity. However, further studies are needed to clarify the suppressive capacity of ILCregs *in vivo* and their specific roles during active inflammation.

In conclusion, the current study identifies a unique anti-inflammatory pathway by which ILC2s are converted to ILCregs by RA. *In vitro*, ILCregs can suppress the proliferation of $CD4^+$ T cells and ILC2s through IL-10 production. ILCregs were induced in the airways during type-2 airway inflammation by interaction of ILC2s with airway epithelial cells at local sites of inflammation, which may contribute to resolution of the allergic airway inflammation. These mechanisms may represent a negative feedback system for maintaining and reestablishing airway homeostasis and avoiding excessive tissue injury and inflammation.

Acknowledgements

We thank the members of SIAF (Dr. Willem van de Veen, Mr. Oliver Wirz, Ms. Anna Globinska, Dr. Barbara Stanic, Dr. Shuo Li and Dr. Milena Sokolowska), and the members of NCCHD (Ms. Masako Fujiwara, Ms. Yoshiko Shimamoto, Ms. Tamiko Sasaki, Mr. Nobuyuki Watanabe, Dr. Mariko Hara, Dr. Akio Matsuda and Ms. Kazue Takeda) for their skilled technical assistance. We also thank the members of IMS (Dr. Ayako Takamori, Dr. Eri Shimura and Ms. Sachiko Yamaguchi) for their invaluable technical assistance. We thank Dr. Jesper Säfholm and Dr. Mamdoh-AI-Ameri, on behalf of ChAMP, for the human lung tissue.

Author Contributions

H.M. designed the study, performed experiments, analyzed the data and wrote the manuscript. T.K., K.S., M.W. and P.W. performed the experiments of primary human bronchial epithelial cells. B.W. performed the immunohistochemistry of human nasal tissues. A.R. performed the experiments on human lung tissues. K. Motomura, M.T., K.O., N.O., K.A., K.S. and S.N. performed the mouse experiments. M.S. provided the human nasal tissues. C.A., F.C.G., G.T. and A.N performed the analysis of RNA-seq. K.S. and K.H. provided mice. J.M. and G.N. designed the human lung tissue experiments. H.S., L.O., K. Matsumoto and M.A. provided insight into the study design. C.A.A. designed and wrote the manuscript.

Figure Legends

FIG 1. Retinoic acid induces IL-10, but not IL-5 or IL-13, in ILC2s through retinoic acid receptor.

A, IL-10 production by human ILC2 lines exposed for 3 days to various types of stimuli in the presence of IL-2 (100 U/ml) and/or IL-33 (50 ng/ml). **B,** Production of cytokines by human ILC2 lines stimulated for 3 days with IL-2 and IL-33 in the presence of different doses of RA. **C,** Production of cytokines by human ILC2 lines stimulated for 3days with IL-2, IL-33 and RA (100nM), in combination with pan-retinoic acid receptor inhibitor (RAi; BMS 493, Tocris Bioscience, Bristol, UK). Data are shown as the mean ± SEM. n = 5 per group in triplicate. *$*P<0.05$, **$*P<0.01$* between indicated groups.

FIG 2. IL-10 producing ILC2s acquire a regulatory phenotype.

A, Gene expression profiling of IL-10^+ ILCs and IL-10^- ILCs induced from ILC2 lines by IL-2, IL-33 and RA. Differentially regulated genes related to ILC2s and Treg cells were selected for heatmap analysis. **B,** Reduced ILC2-related mRNAs in IL-10^+ ILCs induced from ILC2s (fdr<0.01). **C,** Flow cytometric analyses of ILC2-related molecules on IL-10^+ and IL-10^- ILCs induced from ILC2s. **D,** Increased quantitative mRNAs of Treg cell-related molecules in IL-10^+ ILCs compared to IL-10^- counterparts. **E,** Increased expression of Treg cell-related molecules, i.e., CTLA-4 and CD25, on IL-10^+ ILCs by flow cytometry.

FIG 3. IL-10-producing ILCs suppress proliferation of $CD4^+$ T cells and ILC2s through IL-10.

A, Decreased division of carboxyfluorescein succinimidyl ester (CFSE)-labeled $CD4^+$ T cells in the presence of IL-10^+ ILCs at different ratios. **B and C,** Co-culture of

598 CFSE-labeled $CD4^+$ T cells with IL-10^+ ILCs at a 2:1 ratio with anti-IL-10R blocking
599 mAbs (5 μg/ml), anti-CTLA-4 blocking mAbs (5 μg/ml) or isotype control mAbs (5
600 μg/ml). IL-10 (10 ng/ml) was used as a control. **D,** Co-culture of CFSE-labeled ILC2
601 lines with IL-10^+ ILCs at different ratios (indicated in the figure). **E,** Co-culture of
602 CFSE-labeled ILC2 lines with IL-10^+ ILCs at a 2:1 ratio with anti-IL-10R blocking Abs
603 (5 μg/ml) or isotype control Abs (5 μg/ml). IL-10 (10 ng/ml) was used as a control. Cells
604 were harvested after 3 days. The CFSE fluorescence level was analyzed by flow
605 cytometry, and the division index was calculated. Data are shown as the mean ± SEM. n =
606 3 per group in duplicate. *$*P<0.05$, $**P<0.01$, $***P<0.001$* between indicated groups.
607
608 **FIG 4. ILCs in nasal tissues from patients with CRSwNP exhibit a regulatory**
609 **phenotype.**
610 **A and B,** Flow cytometric analysis of ILCs in nasal tissue. Frequency of
611 $CD45^+Lin^-CD127^+CD161^+$IL-$10^+$ cells and frequency of
612 $CD45^+Lin^-CD127^+CD161^+CTLA\text{-}4^+$ cells in nasal tissue from healthy individuals (n = 7)
613 and patients with CRSwNP (n = 7). Each dot represents a single donor. **C,**
614 Immunofluorescence staining of nasal tissues from patients with CRSwNP, showing
615 $CD3^-NCR1^-CD161^+$IL-10^+ ILCs by staining for CD3 and NCR1 (white), CD161 (red),
616 IL-10 (green) and DAPI (blue). **D,** Expression of *ALDH1A1*, *ALDH1A2* and *ALDH1A3*
617 mRNA in nasal tissues from healthy individuals (n = 12) and patients with CRSwNP (n =
618 7). **E,** Immunofluorescence staining of nasal tissues from healthy individuals and patients
619 with CRSwNP, showing the expression of RALDH-1 by staining for RALDH-1 (red) and
620 DAPI (blue). **F,** Expression of *ALDH1A1*, *ALDH1A2* and *ALDH1A3* mRNA in air-liquid
621 interface (ALI) cultures of primary bronchial epithelial cells from healthy individuals (n

= 4) stimulated with various cytokines such as IL-5, IL-13 and IL-33 for 24 h. N.D.: not detected. **G,** Frequency of $CD45^+Lin^-CD161^+IL\text{-}10^+$ in lung mononuclear cells before and after 72 h stimulation with IL-2, IL-33 and RA (n = 5). Each dot represents a single donor. Data are shown as mean ± SEM. **P<0.05, ***P<0.001* between indicated groups.

FIG 5. IL-10 producing ILCs were increased in inflamed lung tissue, but not in mesentery, in an HDM-induced asthma-like model.

A, Numbers of total cells, eosinophils and $CD45^+Lin^-CD127^+KLRG1^+sca\text{-}1^+$ ILC2s. **B,** Frequency of $CD45^+Lin^-IL\text{-}10^+$ cells in BALF and lungs tissues from mice 72 h after last intranasal inhalation (saline, n = 5; and HDM, n = 8). **C,** Quantification of surface molecules on $CD45^+Lin^-IL\text{-}10^+$ cells and $CD45^+Lin^-IL\text{-}10^-$ cells in lungs tissues, assessed by flow cytometry. **D,** Quantification of surface molecules and transcription factors on $CD45^+Lin^-CD90^+IL\text{-}10^+$ cells and $CD45^+Lin^-CD90^+IL\text{-}10^-$ cells in lungs tissues. **E,** Immunofluorescence staining of lung tissue from IL-10 reporter mice after HDM inhalation, showing $IL\text{-}10^+$ ILCs by staining for CD3 (purple), sca-1 (red), IL-10 (green) and DAPI (blue). **F,** Frequencies of $CD45^+Lin^-CD127^+KLRG1^+sca\text{-}1^+$ ILC2s and $CD45^+Lin^-IL\text{-}10^+$ cells in the mesentery from mice 72 h after the last intranasal inhalation (saline, n = 5; and HDM, n = 8). **G,** Immunohistochemistry of RALDH-1 in lung tissues from wild-type mice 72 h after the last intranasal inhalation. Scale bars, 100μm. Data are representative of two independent experiments (saline, n=5; and HDM, n=5).

References

1. Artis D, Spits H. The biology of innate lymphoid cells. Nature 2015;

517:293-301.
2. Mjosberg J, Spits H. Human innate lymphoid cells. J Allergy Clin Immunol 2016; 138:1265-76.
3. Morita H, Moro K, Koyasu S. Innate lymphoid cells in allergic and nonallergic inflammation. J Allergy Clin Immunol 2016; 138:1253-64.
4. Klose CS, Artis D. Innate lymphoid cells as regulators of immunity, inflammation and tissue homeostasis. Nat Immunol 2016; 17:765-74.
5. Kortekaas Krohn I, Shikhagaie MM, Golebski K, Bernink JHJ, Breynaert C, Creyns B, et al. Emerging roles of innate lymphoid cells in inflammatory diseases: clinical implications. Allergy 2017.
6. Morita H, Nakae S, Saito H, Matsumoto K. IL-33 in clinical practice: Size matters? J Allergy Clin Immunol 2017; 140:381-3.
7. Liew FY, Girard JP, Turnquist HR. Interleukin-33 in health and disease. Nat Rev Immunol 2016.
8. Kubo M. Innate and adaptive type 2 immunity in lung allergic inflammation. Immunol Rev 2017; 278:162-72.
9. Morita H, Arae K, Ohno T, Kajiwara N, Oboki K, Matsuda A, et al. ST2 requires Th2-, but not Th17-, type airway inflammation in epicutaneously antigen-sensitized mice. Allergol Int 2012; 61:265-73.
10. Morita H, Arae K, Unno H, Miyauchi K, Toyama S, Nambu A, et al. An Interleukin-33-Mast Cell-Interleukin-2 Axis Suppresses Papain-Induced Allergic Inflammation by Promoting Regulatory T Cell Numbers. Immunity 2015; 43:175-86.
11. Motomura Y, Morita H, Moro K, Nakae S, Artis D, Endo TA, et al. Basophil-derived interleukin-4 controls the function of natural helper cells, a member of ILC2s, in lung inflammation. Immunity 2014; 40:758-71.
12. de Kleer IM, Kool M, de Bruijn MJ, Willart M, van Moorleghem J, Schuijs MJ, et al. Perinatal Activation of the Interleukin-33 Pathway Promotes Type 2 Immunity in the Developing Lung. Immunity 2016; 45:1285-98.
13. Bal SM, Bernink JH, Nagasawa M, Groot J, Shikhagaie MM, Golebski K, et al. IL-1beta, IL-4 and IL-12 control the fate of group 2 innate lymphoid cells in human airway inflammation in the lungs. Nat Immunol 2016; 17:636-45.
14. Mjosberg JM, Trifari S, Crellin NK, Peters CP, van Drunen CM, Piet B, et al. Human IL-25- and IL-33-responsive type 2 innate lymphoid cells are defined by expression of CRTH2 and CD161. Nat Immunol 2011; 12:1055-62.
15. Rigas D, Lewis G, Aron JL, Wang B, Banie H, Sankaranarayanan I, et al. Type 2 innate lymphoid cell suppression by regulatory T cells attenuates airway hyperreactivity and requires inducible T-cell costimulator-inducible T-cell costimulator ligand interaction. J Allergy Clin Immunol 2017; 139:1468-77 e2.
16. Krishnamoorthy N, Burkett PR, Dalli J, Abdulnour RE, Colas R, Ramon S, et al. Cutting edge: maresin-1 engages regulatory T cells to limit type 2 innate lymphoid cell activation and promote resolution of lung inflammation. J Immunol 2015; 194:863-7.
17. Ogasawara N, Poposki JA, Klingler AI, Tan BK, Weibman AR, Hulse KE, et al. IL-10, TGF-beta, and glucocorticoid prevent the production of type 2 cytokines in human group 2 innate lymphoid cells. J Allergy Clin Immunol 2017.
18. Moro K, Kabata H, Tanabe M, Koga S, Takeno N, Mochizuki M, et al. Interferon

693 and IL-27 antagonize the function of group 2 innate lymphoid cells and type 2
694 innate immune responses. Nat Immunol 2016; 17:76-86.
695 19. Duerr CU, McCarthy CD, Mindt BC, Rubio M, Meli AP, Pothlichet J, et al. Type I
696 interferon restricts type 2 immunopathology through the regulation of group 2
697 innate lymphoid cells. Nat Immunol 2016; 17:65-75.
698 20. Molofsky AB, Van Gool F, Liang HE, Van Dyken SJ, Nussbaum JC, Lee J, et al.
699 Interleukin-33 and Interferon-gamma Counter-Regulate Group 2 Innate
700 Lymphoid Cell Activation during Immune Perturbation. Immunity 2015;
701 43:161-74.
702 21. Kudo F, Ikutani M, Seki Y, Otsubo T, Kawamura YI, Dohi T, et al.
703 Interferon-gamma constrains cytokine production of group 2 innate lymphoid
704 cells. Immunology 2016; 147:21-9.
705 22. Zhou W, Toki S, Zhang J, Goleniewksa K, Newcomb DC, Cephus JY, et al.
706 Prostaglandin I2 Signaling and Inhibition of Group 2 Innate Lymphoid Cell
707 Responses. Am J Respir Crit Care Med 2016; 193:31-42.
708 23. Barnig C, Cernadas M, Dutile S, Liu X, Perrella MA, Kazani S, et al. Lipoxin A4
709 regulates natural killer cell and type 2 innate lymphoid cell activation in asthma.
710 Sci Transl Med 2013; 5:174ra26.
711 24. Wang S, Xia P, Chen Y, Qu Y, Xiong Z, Ye B, et al. Regulatory Innate Lymphoid
712 Cells Control Innate Intestinal Inflammation. Cell 2017; 171:201-16 e18.
713 25. Ravindran A, Ronnberg E, Dahlin JS, Mazzurana L, Safholm J, Orre AC, et al. An
714 Optimized Protocol for the Isolation and Functional Analysis of Human Lung
715 Mast Cells. Front Immunol 2018; 9:2193.
716 26. Atarashi K, Tanoue T, Shima T, Imaoka A, Kuwahara T, Momose Y, et al.
717 Induction of colonic regulatory T cells by indigenous Clostridium species.
718 Science 2011; 331:337-41.
719 27. Tanoue T, Atarashi K, Honda K. Development and maintenance of intestinal
720 regulatory T cells. Nat Rev Immunol 2016; 16:295-309.
721 28. Bernink JH, Krabbendam L, Germar K, de Jong E, Gronke K, Kofoed-Nielsen M,
722 et al. Interleukin-12 and -23 Control Plasticity of CD127(+) Group 1 and Group 3
723 Innate Lymphoid Cells in the Intestinal Lamina Propria. Immunity 2015;
724 43:146-60.
725 29. Bernink JH, Peters CP, Munneke M, te Velde AA, Meijer SL, Weijer K, et al.
726 Human type 1 innate lymphoid cells accumulate in inflamed mucosal tissues. Nat
727 Immunol 2013; 14:221-9.
728 30. Lim AI, Menegatti S, Bustamante J, Le Bourhis L, Allez M, Rogge L, et al. IL-12
729 drives functional plasticity of human group 2 innate lymphoid cells. J Exp Med
730 2016; 213:569-83.
731 31. Ohne Y, Silver JS, Thompson-Snipes L, Collet MA, Blanck JP, Cantarel BL, et al.
732 IL-1 is a critical regulator of group 2 innate lymphoid cell function and plasticity.
733 Nat Immunol 2016; 17:646-55.
734 32. Silver JS, Kearley J, Copenhaver AM, Sanden C, Mori M, Yu L, et al.
735 Inflammatory triggers associated with exacerbations of COPD orchestrate
736 plasticity of group 2 innate lymphoid cells in the lungs. Nat Immunol 2016;
737 17:626-35.
738 33. Coombes JL, Siddiqui KR, Arancibia-Carcamo CV, Hall J, Sun CM, Belkaid Y, et
739 al. A functionally specialized population of mucosal CD103+ DCs induces

Foxp3+ regulatory T cells via a TGF-beta and retinoic acid-dependent mechanism. J Exp Med 2007; 204:1757-64.

34. Sun CM, Hall JA, Blank RB, Bouladoux N, Oukka M, Mora JR, et al. Small intestine lamina propria dendritic cells promote de novo generation of Foxp3 T reg cells via retinoic acid. J Exp Med 2007; 204:1775-85.

35. Kang SW, Kim SH, Lee N, Lee WW, Hwang KA, Shin MS, et al. 1,25-Dihyroxyvitamin D3 promotes FOXP3 expression via binding to vitamin D response elements in its conserved noncoding sequence region. J Immunol 2012; 188:5276-82.

36. Kastner P, Lawrence HJ, Waltzinger C, Ghyselinck NB, Chambon P, Chan S. Positive and negative regulation of granulopoiesis by endogenous RARalpha. Blood 2001; 97:1314-20.

37. Bjorklund AK, Forkel M, Picelli S, Konya V, Theorell J, Friberg D, et al. The heterogeneity of human CD127(+) innate lymphoid cells revealed by single-cell RNA sequencing. Nat Immunol 2016; 17:451-60.

38. Sugita K, Steer CA, Martinez-Gonzalez I, Altunbulakli C, Morita H, Castro-Giner F, et al. Type 2 innate Lymphoid Cells Disrupt Bronchial Epithelial Barrier Integrity by Targeting Tight Junctions Via IL-13 in Asthma. J Allergy Clin Immunol 2017; 141:300-10.

39. Li BW, de Bruijn MJ, Tindemans I, Lukkes M, KleinJan A, Hoogsteden HC, et al. T cells are necessary for ILC2 activation in house dust mite-induced allergic airway inflammation in mice. Eur J Immunol 2016; 46:1392-403.

40. Oboki K, Ohno T, Kajiwara N, Arae K, Morita H, Ishii A, et al. IL-33 is a crucial amplifier of innate rather than acquired immunity. Proc Natl Acad Sci U S A 2010; 107:18581-6.

41. Moro K, Ealey KN, Kabata H, Koyasu S. Isolation and analysis of group 2 innate lymphoid cells in mice. Nat Protoc 2015; 10:792-806.

42. Moro K, Yamada T, Tanabe M, Takeuchi T, Ikawa T, Kawamoto H, et al. Innate production of T(H)2 cytokines by adipose tissue-associated c-Kit(+)Sca-1(+) lymphoid cells. Nature 2010; 463:540-4.

43. Gasteiger G, Fan X, Dikiy S, Lee SY, Rudensky AY. Tissue residency of innate lymphoid cells in lymphoid and nonlymphoid organs. Science 2015; 350:981-5.

44. Bono MR, Tejon G, Flores-Santibanez F, Fernandez D, Rosemblatt M, Sauma D. Retinoic Acid as a Modulator of T Cell Immunity. Nutrients 2016; 8:E349.

45. Mucida D, Pino-Lagos K, Kim G, Nowak E, Benson MJ, Kronenberg M, et al. Retinoic acid can directly promote TGF-beta-mediated Foxp3(+) Treg cell conversion of naive T cells. Immunity 2009; 30:471-2; author reply 2-3.

46. Benson MJ, Pino-Lagos K, Rosemblatt M, Noelle RJ. All-trans retinoic acid mediates enhanced T reg cell growth, differentiation, and gut homing in the face of high levels of co-stimulation. J Exp Med 2007; 204:1765-74.

47. Kim MH, Taparowsky EJ, Kim CH. Retinoic Acid Differentially Regulates the Migration of Innate Lymphoid Cell Subsets to the Gut. Immunity 2015; 43:107-19.

48. Mielke LA, Jones SA, Raverdeau M, Higgs R, Stefanska A, Groom JR, et al. Retinoic acid expression associates with enhanced IL-22 production by gammadelta T cells and innate lymphoid cells and attenuation of intestinal inflammation. J Exp Med 2013; 210:1117-24.

49. Spencer SP, Wilhelm C, Yang Q, Hall JA, Bouladoux N, Boyd A, et al. Adaptation of innate lymphoid cells to a micronutrient deficiency promotes type 2 barrier immunity. Science 2014; 343:432-7.
50. van de Pavert SA, Ferreira M, Domingues RG, Ribeiro H, Molenaar R, Moreira-Santos L, et al. Maternal retinoids control type 3 innate lymphoid cells and set the offspring immunity. Nature 2014; 508:123-7.
51. Goverse G, Labao-Almeida C, Ferreira M, Molenaar R, Wahlen S, Konijn T, et al. Vitamin A Controls the Presence of RORgamma+ Innate Lymphoid Cells and Lymphoid Tissue in the Small Intestine. J Immunol 2016; 196:5148-55.
52. Trabanelli S, Chevalier MF, Martinez-Usatorre A, Gomez-Cadena A, Salome B, Lecciso M, et al. Tumour-derived PGD2 and NKp30-B7H6 engagement drives an immunosuppressive ILC2-MDSC axis. Nat Commun 2017; 8:593.
53. Seehus CR, Kadavallore A, Torre B, Yeckes AR, Wang Y, Tang J, et al. Alternative activation generates IL-10 producing type 2 innate lymphoid cells. Nat Commun 2017; 8:1900.
54. Dawson HD, Collins G, Pyle R, Key M, Weeraratna A, Deep-Dixit V, et al. Direct and indirect effects of retinoic acid on human Th2 cytokine and chemokine expression by human T lymphocytes. BMC Immunol 2006; 7:27.
55. Wansley DL, Yin Y, Prussin C. The retinoic acid receptor-alpha modulators ATRA and Ro415253 reciprocally regulate human IL-5+ Th2 cell proliferation and cytokine expression. Clin Mol Allergy 2013; 11:4.
56. Goswami S, Angkasekwinai P, Shan M, Greenlee KJ, Barranco WT, Polikepahad S, et al. Divergent functions for airway epithelial matrix metalloproteinase 7 and retinoic acid in experimental asthma. Nat Immunol 2009; 10:496-503.
57. Simoni Y, Fehlings M, Kloverpris HN, McGovern N, Koo SL, Loh CY, et al. Human Innate Lymphoid Cell Subsets Possess Tissue-Type Based Heterogeneity in Phenotype and Frequency. Immunity 2017; 46:148-61.
58. Lim AI, Li Y, Lopez-Lastra S, Stadhouders R, Paul F, Casrouge A, et al. Systemic Human ILC Precursors Provide a Substrate for Tissue ILC Differentiation. Cell 2017; 168:1086-100 e10.

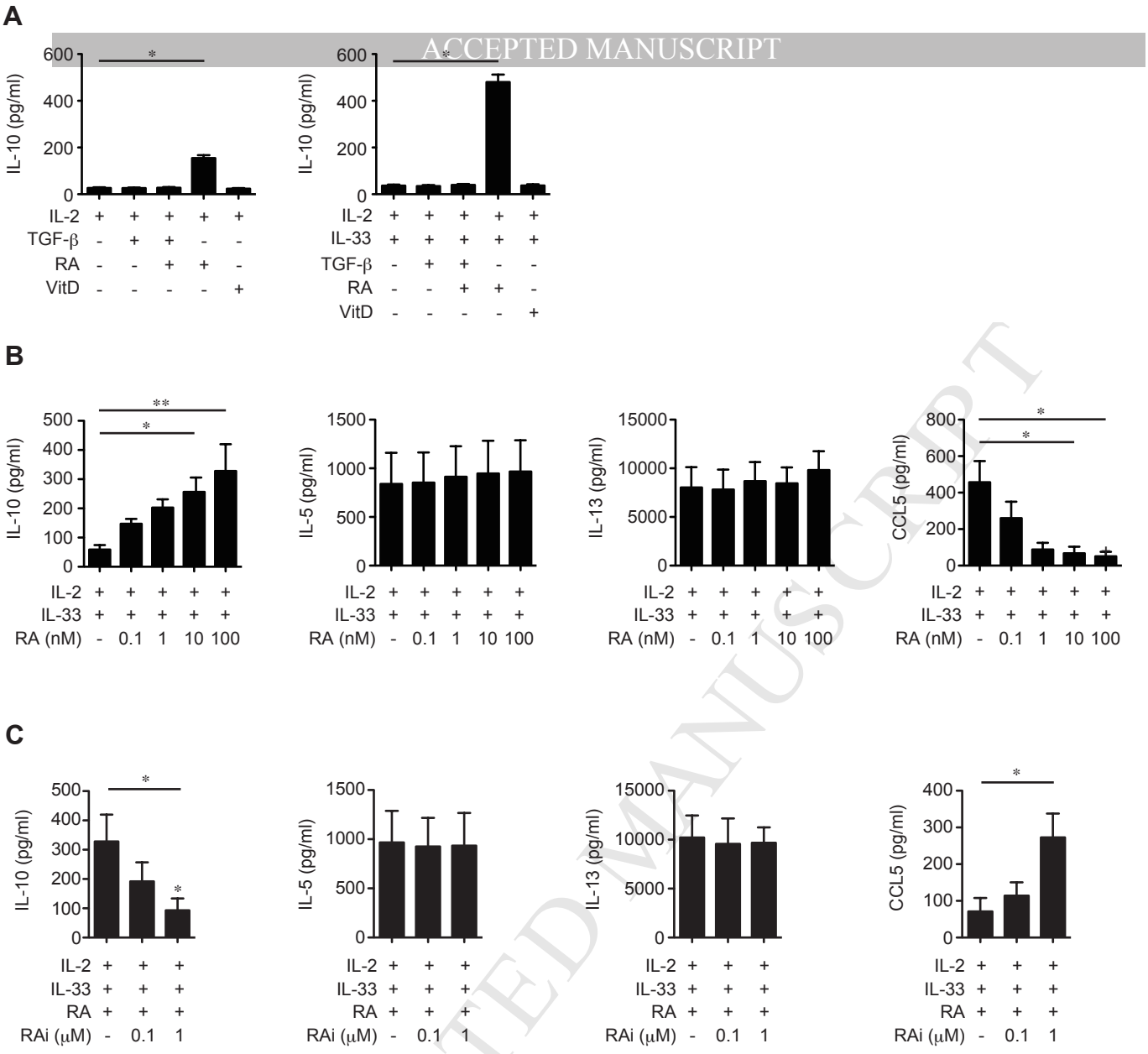

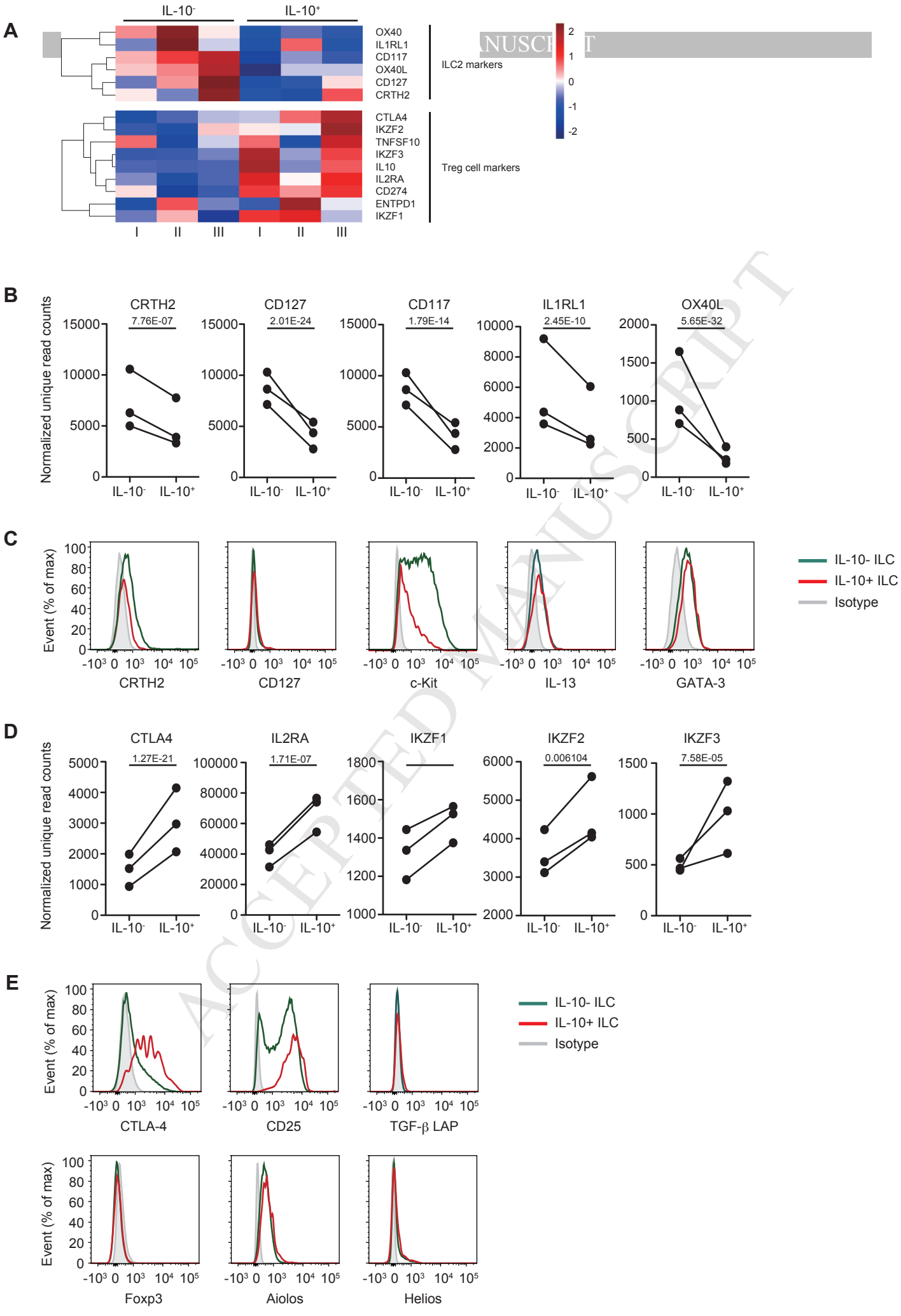

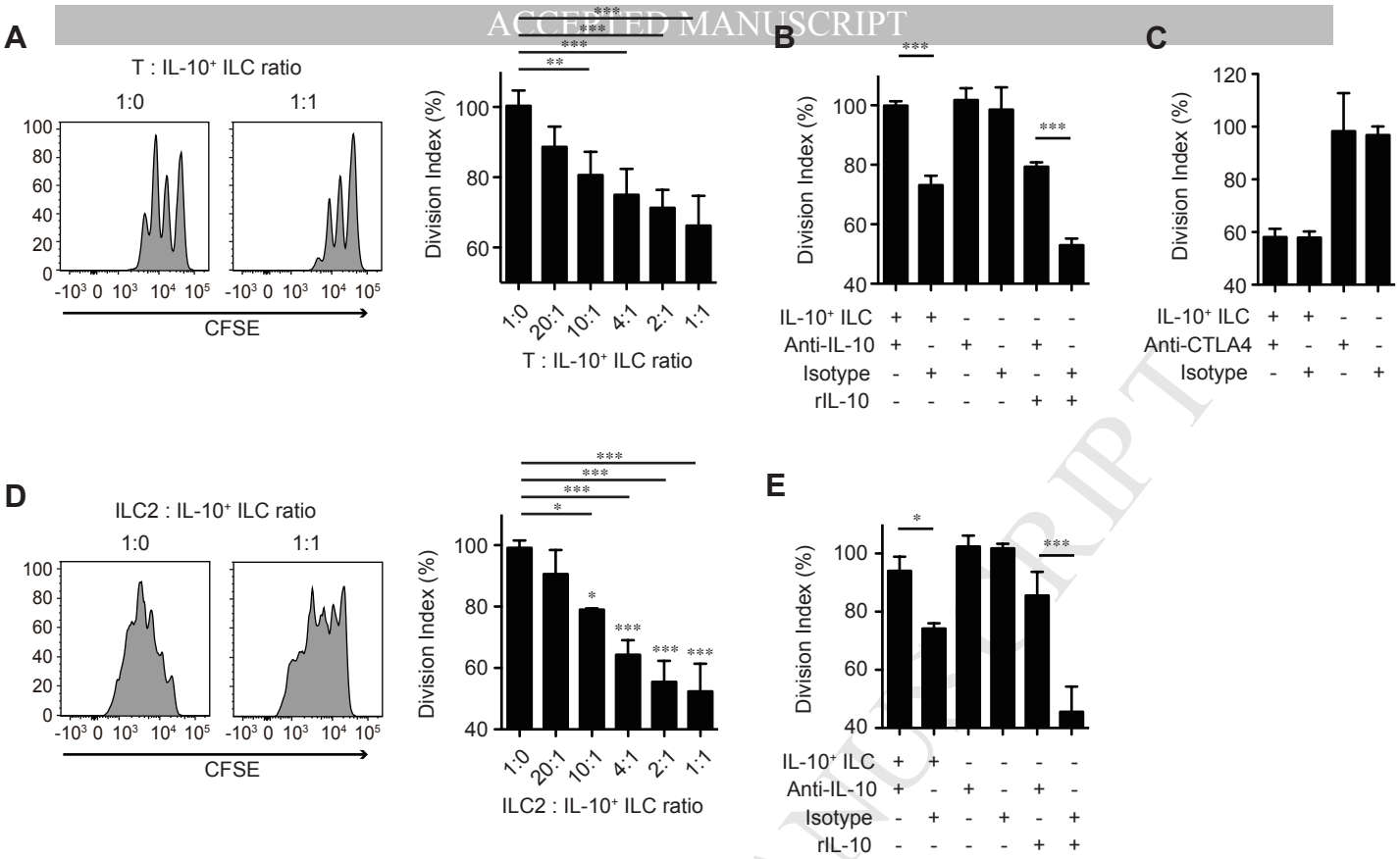

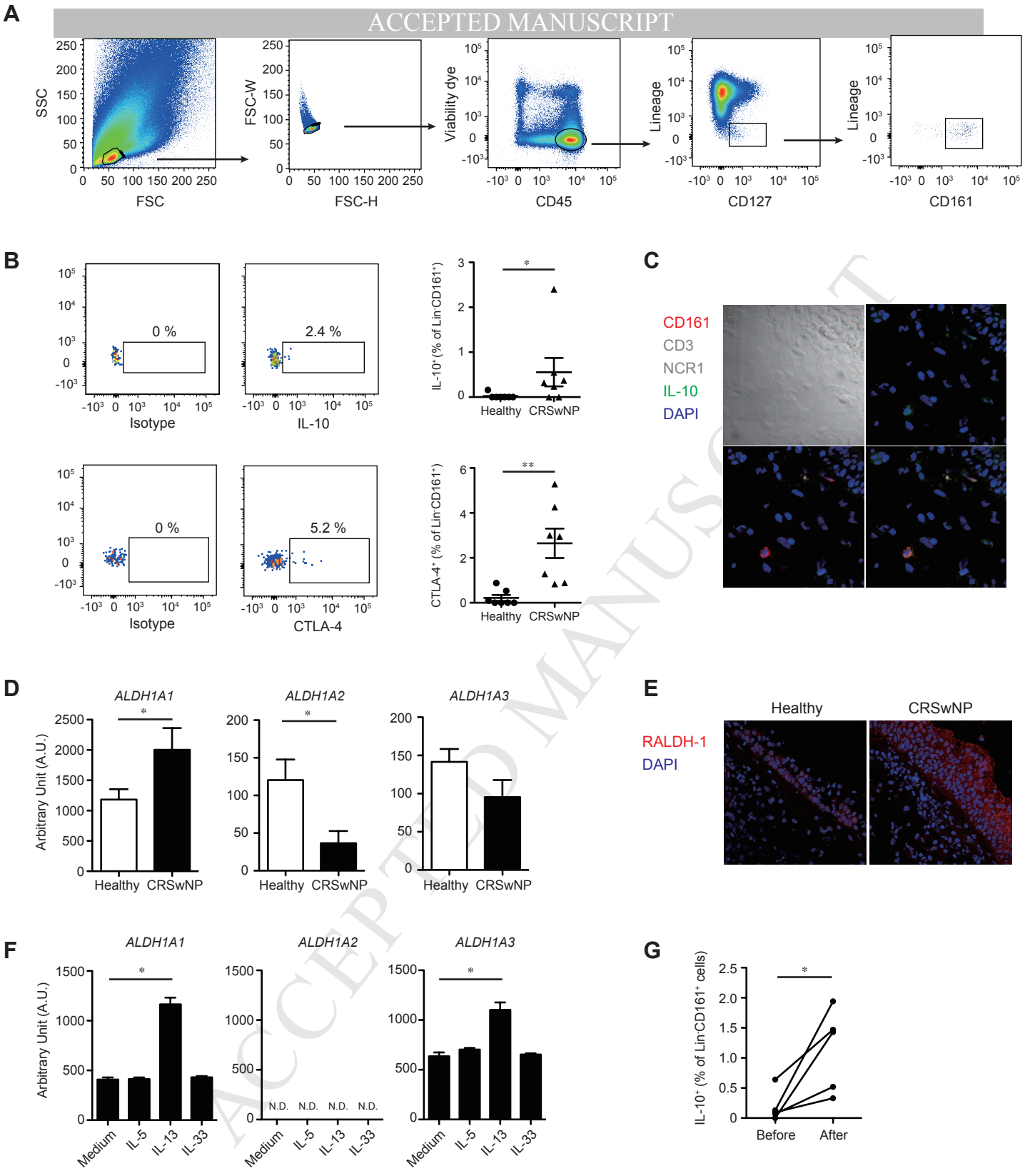

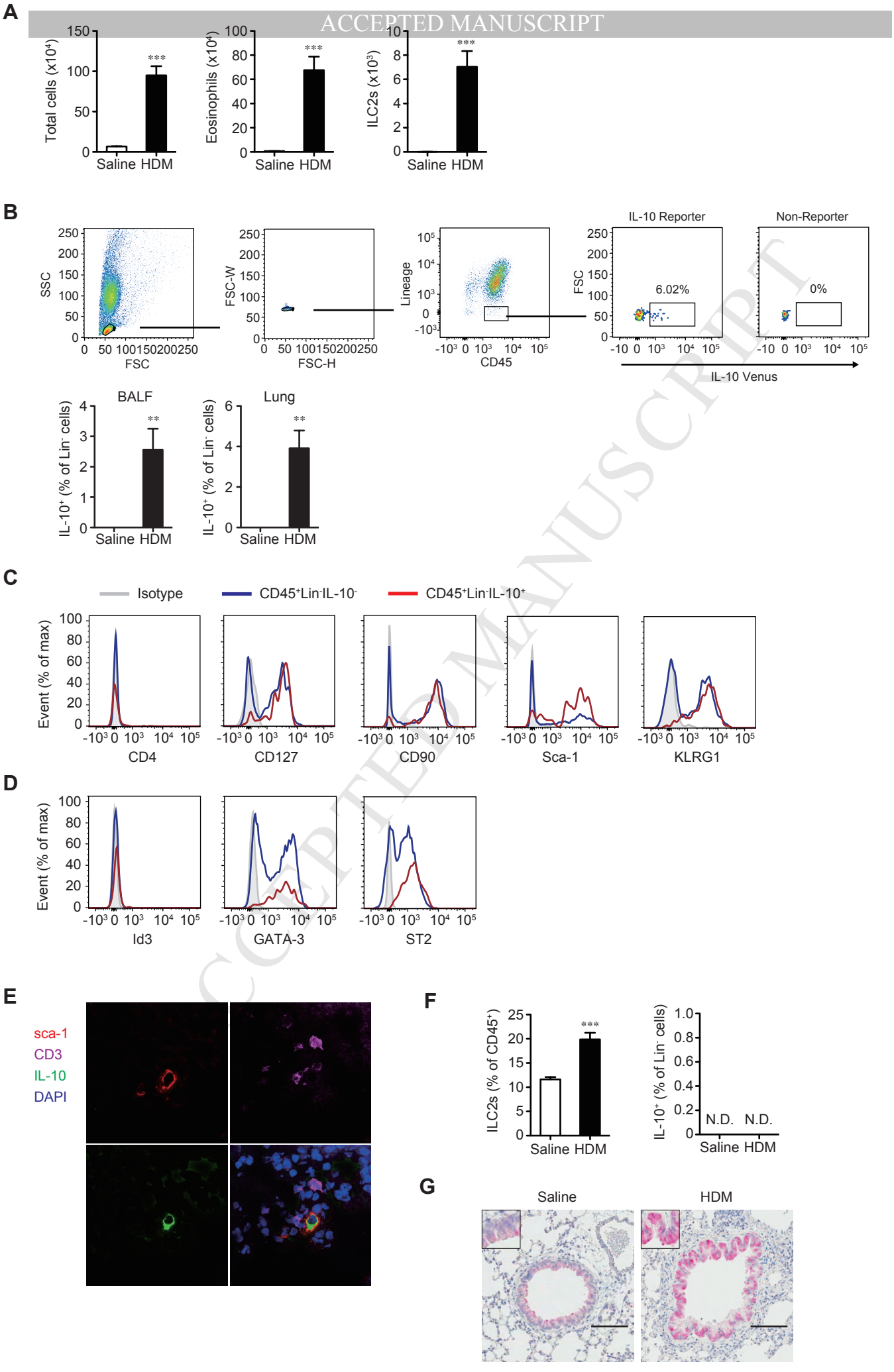

Supplementary Table E1 Top 50 upregulated genes in IL-10$^+$ ILCs compared to IL-10$^-$ ILCs

	Gene ID	Gene Name	Description	Log2 Ratio	p-Value
1	ENSG00000136634	IL10	interleukin 10	7.018	1.12E-314
2	ENSG00000172348	RCAN2	regulator of calcineurin 2	2.59	1.19E-06
3	ENSG00000106066	CPVL	carboxypeptidase, vitellogenic-like	2.563	5.58E-07
4	ENSG00000186919	ZACN	zinc activated ligand-gated ion channel	2.489	2.02E-07
5	ENSG00000159307	SCUBE1	signal peptide, CUB domain, EGF-like 1	2.405	1.51E-08
6	ENSG00000142303	ADAMTS10	ADAM metallopeptidase with thrombospondin type 1 motif, 10	2.116	0.0006577
7	ENSG00000137558	PI15	peptidase inhibitor 15	2.076	4.90E-06
8	ENSG00000167037	SGSM1	small G protein signaling modulator 1	2.067	8.25E-13
9	ENSG00000060140	STYK1	serine/threonine/tyrosine kinase 1	2.061	0.001257
10	ENSG00000139174	PRICKLE1	prickle homolog 1 (Drosophila)	2.046	0.001768
11	ENSG00000105392	CRX	cone-rod homeobox	2.008	0.001892
12	ENSG00000050730	TNIP3	TNFAIP3 interacting protein 3	1.93	1.72E-09
13	ENSG00000196208	GREB1	growth regulation by estrogen in breast cancer 1	1.867	0.0003084
14	ENSG00000100600	LGMN	legumain	1.783	4.29E-15
15	ENSG00000102048	ASB9	ankyrin repeat and SOCS box containing 9	1.762	2.02E-10
16	ENSG00000069535	MAOB	monoamine oxidase B	1.697	4.47E-12
17	ENSG00000108797	CNTNAP1	contactin associated protein	1.579	0.0007228

			1		
18	ENSG00000006468	ETV1	ets variant 1	1.578	0.001964
19	ENSG00000123689	G0S2	G0/G1switch 2	1.502	7.54E-09
20	ENSG00000164287	CDC20B	cell division cycle 20B	1.48	0.0005164
21	ENSG00000114757	PEX5L	peroxisomal biogenesis factor 5-like	1.444	0.001307
22	ENSG00000171246	NPTX1	neuronal pentraxin I	1.428	4.01E-05
23	ENSG00000183508	FAM46C	family with sequence similarity 46, member C	1.424	3.38E-21
24	ENSG00000145839	IL9	interleukin 9	1.392	1.52E-16
25	ENSG00000176595	KBTBD11	kelch repeat and BTB (POZ) domain containing 11	1.381	9.63E-16
26	ENSG00000125266	EFNB2	ephrin-B2	1.369	0.001467
27	ENSG00000162367	TAL1	T-cell acute lymphocytic leukemia 1	1.339	2.76E-06
28	ENSG00000143195	ILDR2	immunoglobulin-like domain containing receptor 2	1.33	0.0008892
29	ENSG00000171132	PRKCE	protein kinase C, epsilon	1.323	6.60E-22
30	ENSG00000125845	BMP2	bone morphogenetic protein 2	1.308	5.15E-07
31	ENSG00000006075	CCL3	chemokine (C-C motif) ligand 3	1.262	0.0002122
32	ENSG00000113520	IL4	interleukin 4	1.256	2.46E-14
33	ENSG00000144645	OSBPL10	oxysterol binding protein-like 10	1.239	2.23E-06
34	ENSG00000174804	FZD4	frizzled family receptor 4	1.237	0.0001337
35	ENSG00000178184	PARD6G	par-6 family cell polarity regulator gamma	1.225	1.47E-07
36	ENSG00000165029	ABCA1	ATP-binding cassette, sub-family A (ABC1),	1.224	0.0005601

			member 1		
37			C-type lectin domain		
	ENSG00000197992	CLEC9A	family 9, member A	1.19	0.0009048
38			chemokine (C-C motif)		
	ENSG00000121807	CCR2	receptor 2	1.182	8.19E-16
39			chemokine (C-C motif)		
	ENSG00000173585	CCR9	receptor 9	1.169	6.38E-06
40			lin-7 homolog A (C.		
	ENSG00000111052	LIN7A	elegans)	1.161	1.93E-05
41			D4, zinc and double PHD		
	ENSG00000205683	DPF3	fingers, family 3	1.159	0.0009757
42			chemokine (C-C motif)		
	ENSG00000183625	CCR3	receptor 3	1.157	0.0001433
43			C-type lectin domain		
	ENSG00000172243	CLEC7A	family 7, member A	1.147	0.0001114
44	ENSG00000099250	NRP1	neuropilin 1	1.129	4.68E-06
45			FERM domain containing		
	ENSG00000114541	FRMD4B	4B	1.124	7.67E-16
46			fibroblast growth factor		
	ENSG00000066468	FGFR2	receptor 2	1.123	0.0002789
47	ENSG00000120075	HOXB5	homeobox B5	1.092	0.0001196
48			retinol dehydrogenase 12		
	ENSG00000139988	RDH12	(all-trans/9-cis/11-cis)	1.07	0.0009588
49			cytotoxic		
			T-lymphocyte-associated		
	ENSG00000163599	CTLA4	protein 4	1.055	7.03E-25
50	ENSG00000127318	IL22	interleukin 22	1.053	6.75E-15

Supplementary table E2. Sequences of primers designed in house.

Gene	Forward (5'-3')	Reverse (5'-3')
EF1a	CTG AAC CAT CCA GGC CAA AT	GCC GTG TGG CAA TCC AAT
ALDH1A1	CTG CCG GGA AAA GCA ATC	AAA TTC AAC AGC ATT GTC CAA GTC
ALDH1A2	AGG GCA GTT CTT GCA ACC AT	GCG TAA TAT CGA AAG GTT TTG ATG A
ALDH1A3	GTC TGG AAC GGT CTG GAT CAA	CGT ATT CAC CTA GTT CTC TGC CAT

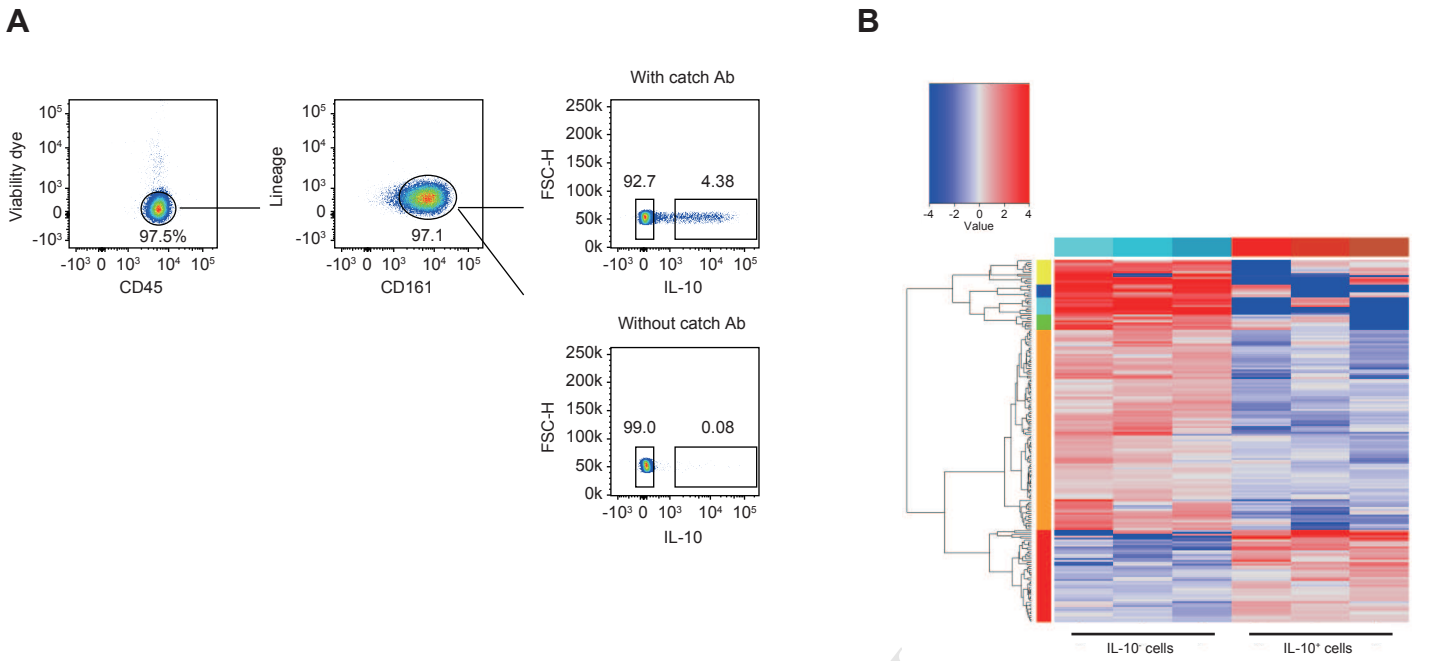

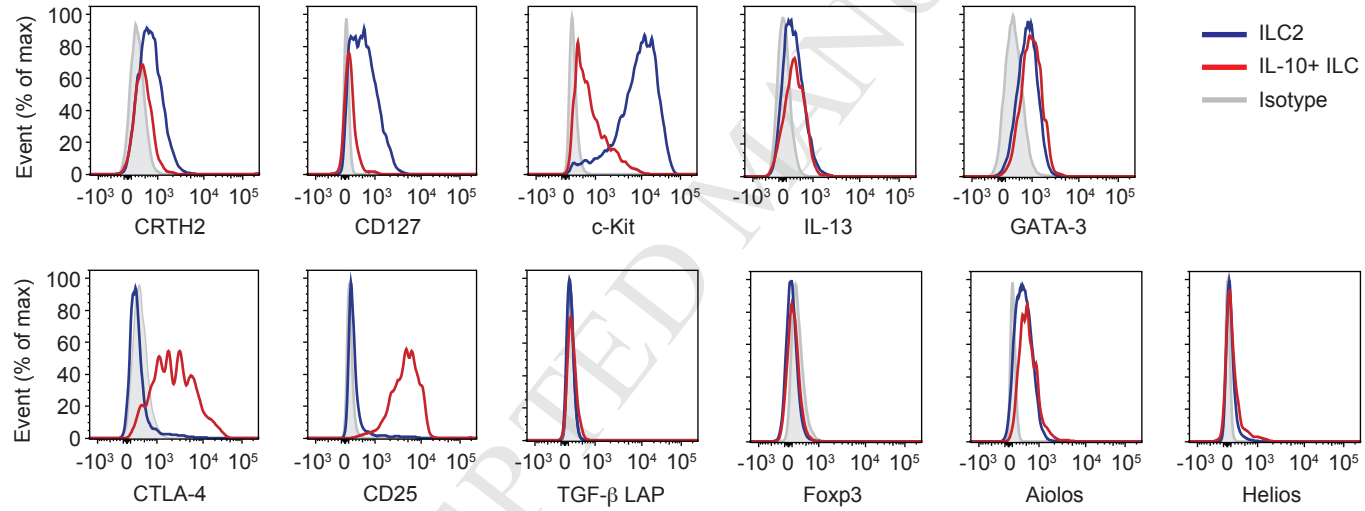

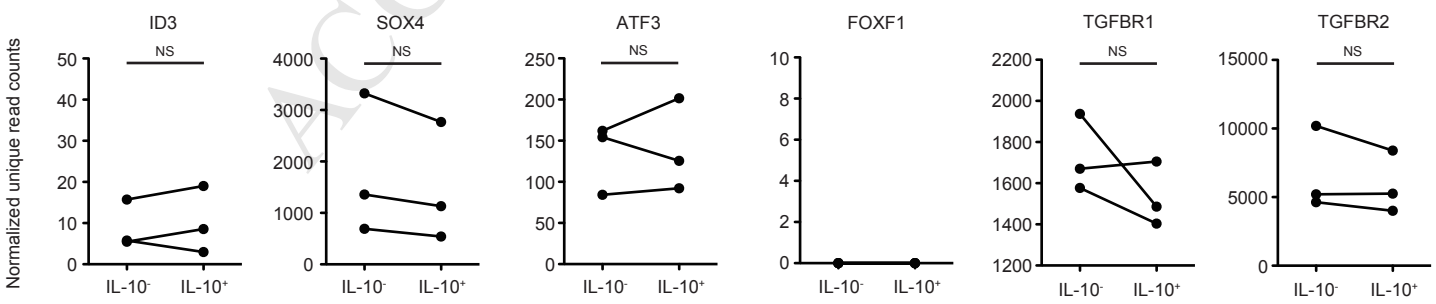

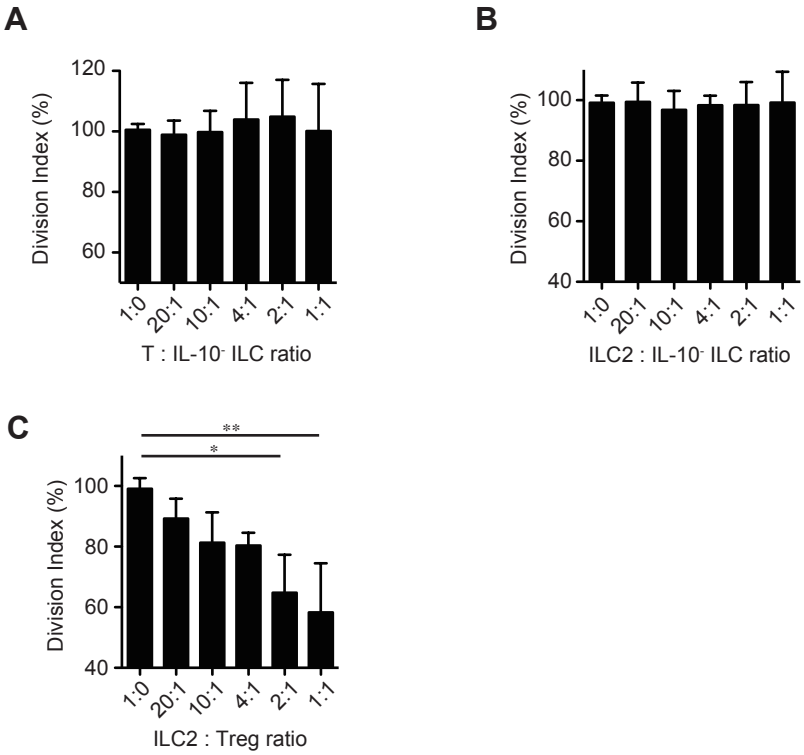

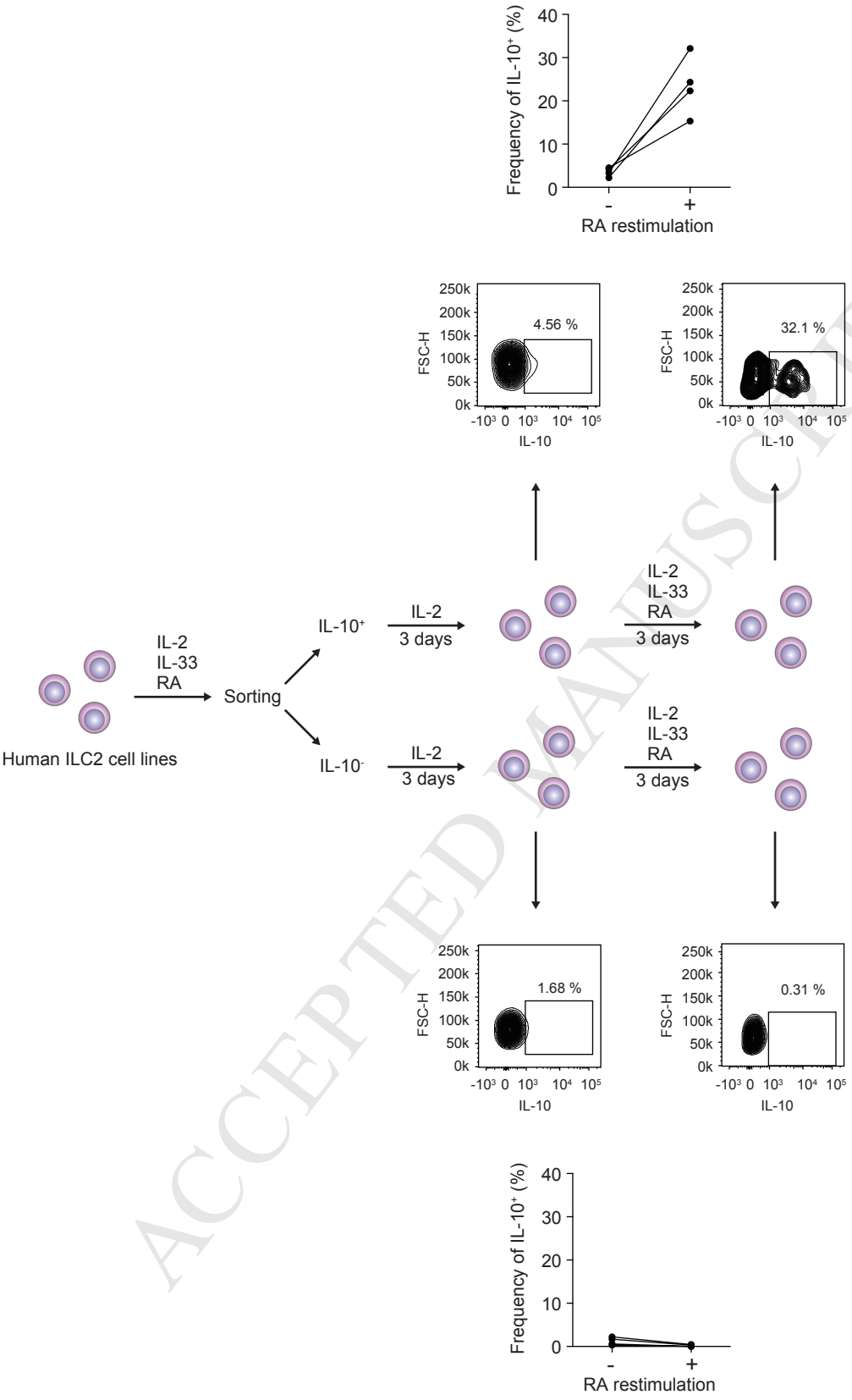

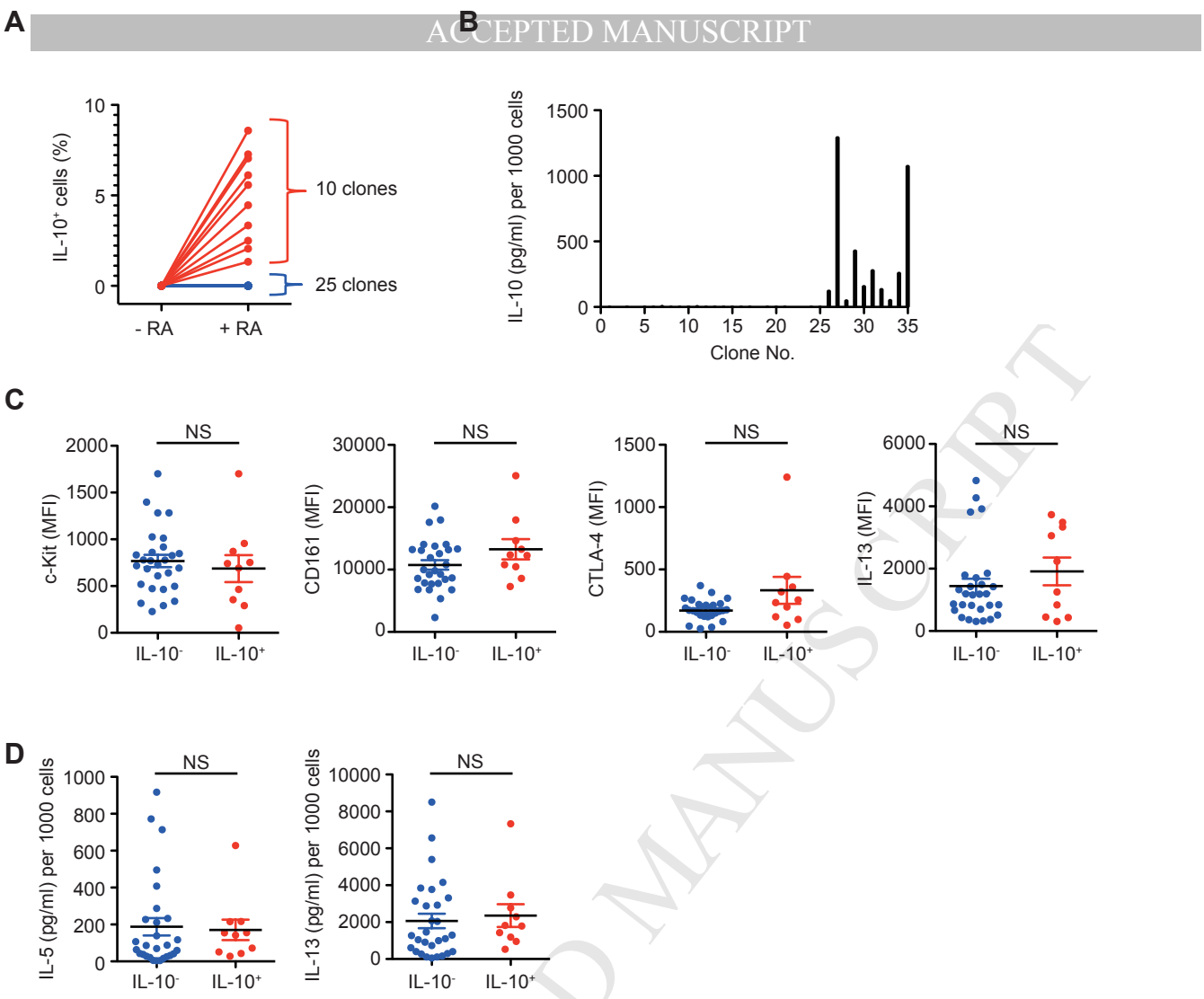

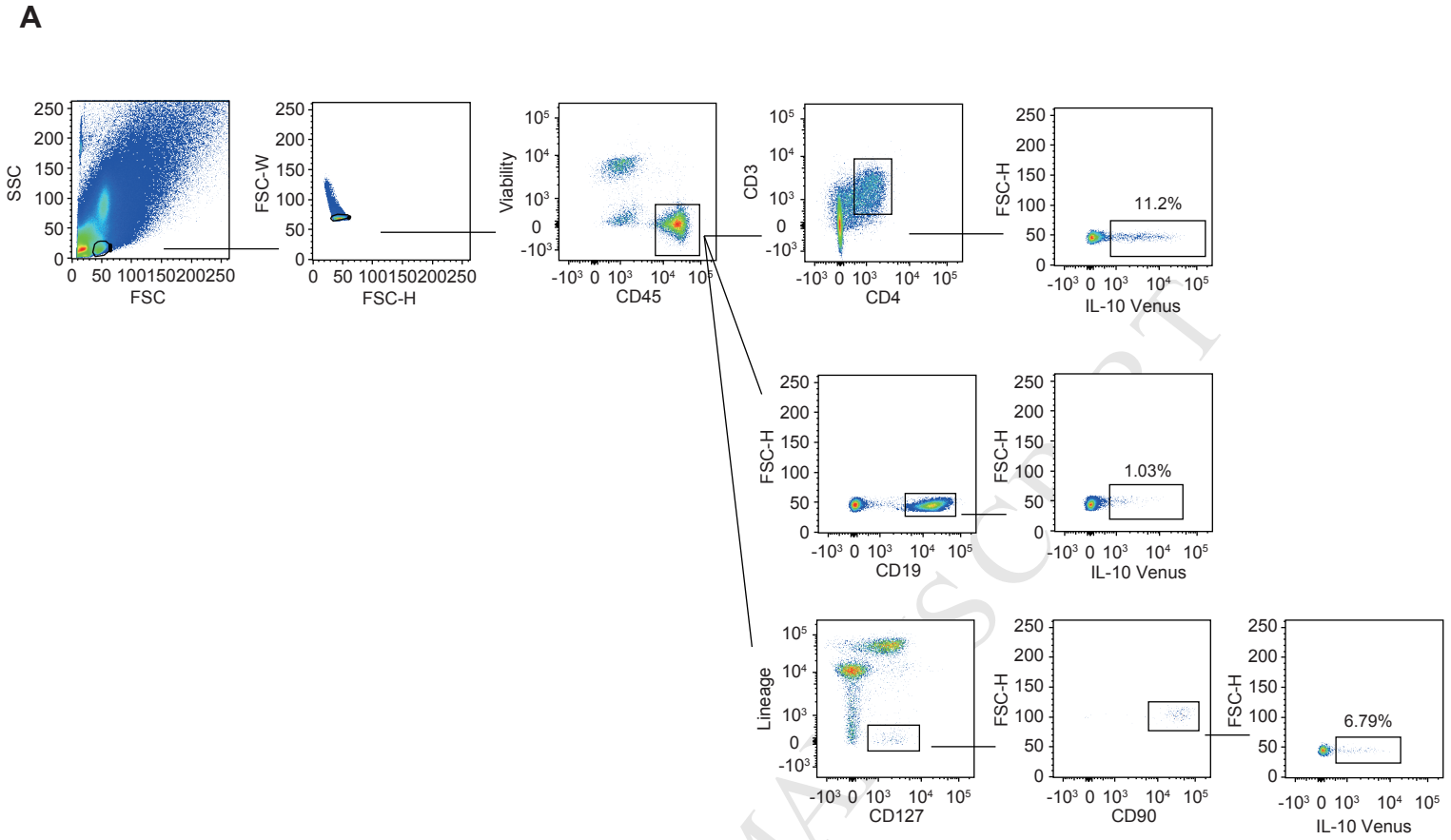

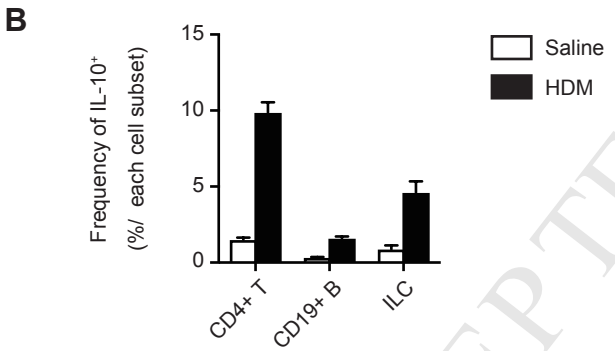

Online methods

Flow cytometry analysis

The following antibodies against human proteins were used for flow cytometry analysis. Fluorescein isothiocyanate (FITC)-conjugated lineage markers: anti-CD1a (HI149), anti-CD3 (OKT3), anti-CD11c (3.9), anti-CD14 (HCD14), anti-CD16 (3G8), anti-CD19 (HIB19), anti-CD34 (581), anti-CD94 (DX22), anti-CD123 (6H6), anti-CD303 (201A), anti-TCRαβ (IP26), anti-TCRγδ (B1), anti-FcεR1α (AER-37), APC-conjugated anti-CLTA-4 (L3D10), PE/Dazzle 594 anti-Foxp3 (206D), PE-Cy7-conjugated anti-CD127 (A019D5), anti-IL-10 (JES3-9D7), anti-Helios (22F6), PerCP/Cy5.5-conjugated anti-CD25 (BC96), anti-GATA3 (16E10A23), anti-CD161 (HP-3G10), Brilliant Violet 421-conjugated anti-CD117 (104D2), anti-LAP (TW4-2F8) and Brilliant Violet 510-conjugated anti-CD45 (HI30) (all from BioLegend, San Diego, CA); and phycoerythrin (PE)-conjugated anti-OX40L (ik-1), Alexa Flour 647-conjugated anti-CD294 (BM16), Brilliant violet 421-conjugated anti-IL-13 (JES10-5A2) and anti-Aiolos (S50-895) (all from BD Biosciences). The following antibodies to mouse proteins were used for flow cytometry analysis. Purified anti-CD16/32 (2.4G2); PE-conjugated lineage markers: anti-CD3e (145-2C11), anti-CD4 (GK1.5), anti-CD8 (53-6.7), anti-CD19 (1D3), anti-B220 (16A), anti-CD49b (DX5) and anti-γδTCR (GL3) (all from BD Biosciences); anti-CD11b (M1/70), anti-CD11c (HL3) and anti-Gr1 (RB6-8C5) (all from BioLegend); and anti-FceR1a (MAR-1) (Thermo Fisher Scientific, Waltham, MA), PE/Cy7-conjugated anti-CD127 (A7R34), APC-conjugated anti-Sca-1 (E13-161.7) and Brilliant Violet 421-conjugated

anti-KLRG1 (2F1/KLRG1) (all from BioLegend). For intracellular cytokine staining, the cells were stimulated for 5 hours with 25 ng/ml PMA (Sigma-Aldrich) plus 1 μg/ml Ionomycin (Sigma-Aldrich) in the presence of 10 μg/ml Brefeldin A (Sigma-Aldrich) for the final 3 hours of culture, and subsequently fixed and stained using a Cytofix/Cytoperm kit Kit (BD biosciences). For staining of transcription factors, the Foxp3 Fix/Perm Buffer set (BioLegend) was used.

IL-10 secretion assay

Live IL-10^+ ILCs and IL-10^- ILCs were isolated using an IL-10 secretion assay (Miltenyi Biotec) and a cell sorter, ARIA II (BD Biosciences). In brief, the ILC2s were stimulated with IL-2, IL-33 and RA. After 2 days' culture at 37°C, cells were restimulated with IL-2, IL-33 and RA and cultured for another 8 h. The cells were then harvested and labeled with Catch Reagent for 5 min at a concentration of 10^8 cells/ml in ice-cold Yssel's medium supplemented with 1% human AB serum. The cells were diluted in warmed-up medium to a final concentration of 10^6 cells/ml and incubated at 37°C for 3 h under slow continuous rotation on the MACSmix tube rotator (Miltenyi Biotec). After incubation, the cells were washed with ice-cold buffer containing 0.5% BSA and 2mM EDTA (Sigma-Aldrich, St. Louis, MO) in PBS and resuspended at a concentration of 10^8 cells/ml in ice-cold buffer. The cells were then stained with detection antibody for 10 min on ice followed by staining of surface lineage markers. Lin^- IL-10^+ cells and Lin^- IL-10^- cells were sorted using a FACS ARIA cell sorter (BD Biosciences).

Suppression assay

For T-cell suppression assay, $CD4^+$ T cells were isolated with an AutoMACS (Miltenyi Biotec) using a human $CD4^+$ T cell Isolation Kit (Miltenyi Biotec) according to the manufacturer's instructions. IL-10^+ and IL-10^- ILCs were co-cultured with carboxy-fluorescein succinimidyl ester (CFSE)-labeled autologous $CD4^+$ T cells at different ratios (total number of cells: 7.5 x 10^4 cells) in the presence of 1 x 10^5 irradiated autologous PBMCs and 2.5 μg/ml of anti-CD3 antibody (OKT3; Thermo Fisher Scientific) in a 96-well half-area plate (Corning) for 3 days. For ILC2 suppression assay, a Lin^- $CRTH2^+$ ILC2 line was sorted with a FACS ARIA II cell sorter (BD Biosciences). IL-10^+ and IL-10^- ILCs were co-cultured with CFSE-labeled autologous ILC2 lines at different ratios (total number of cells: 7.5 x 10^4 cells) in the presence of 1 x 10^5 irradiated autologous PBMCs and 100 U/ml of recombinant human IL-2 (Proleukin, Novartis, Basel, Switzerland) in a 96-well half-area plate (Corning) for 3 days. For suppression assay using Treg cells, $CD4^+CD25^+CD127^{dim/-}$ Treg cells were sorted with a FACS ARIA II cell sorter after enrichment of $CD4^+$ T cells with an AutoMACS using a human $CD4^+$ T cell Isolation Kit (Miltenyi Biotec). Treg cells were co-cultured with CFSE-labeled autologous ILC2 lines at different ratios (total number of cells: 7.5 x 10^4 cells) in the presence of 1 x 10^5 irradiated autologous PBMCs, 2.5 μg/ml of anti-CD3 antibody (OKT3; Thermo Fisher Scientific) and 100 U/ml of recombinant human IL-2 (Proleukin) in a 96-well half-area plate (Corning) for 3 days. The average number of cell divisions were determined as a division index using Flowjo®, and each index was subsequently normalized to the mean of the division index at a 1:0 ratio.

Immunohistochemistry

To stain IL-10$^+$ ILCs in human nasal tissues, nasal tissue specimens from patients with CRSwNP and healthy individuals were embedded in optimum cutting temperature (OCT) compound (Sakura Finetek, Tokyo, Japan) and stored at -80°C until use. 7-μm-thick sections were placed on glass slides and fixed for 7 min at room temperature in 4% (wt/vol) paraformaldehyde (PFA) in PBS. After three washes in PBS, the sections were blocked and made permeable in PBS containing 1% (wt/vol) BSA (Sigma-Aldrich), 10% (vol/vol) normal human serum (Sigma-Aldrich), 20 mg/ml human IgG (Sigma-Aldrich) and 0.1% (vol/vol) Triton X-100, followed by use of an Image-iT^{TM} FX signal enhancer (Thermo Fisher Scientific). For detection of IL-10-producing ILCs, sections were incubated with mouse anti-human CD161 Ab (DX12; BD Biosciences), anti-human NCR1 Ab (MM0491-8F24; Abcam, Cambridge, UK), anti-human IL-10 polyclonal Ab (R&D System, Minneapolis, MN) or corresponding isotype controls such as mouse IgG1, mouse IgG2b (Agilent, Santa Clara, CA) and Goat IgG (Jackson ImmunoResearch, West Grove, PA), followed by incubation with Alexa Fluor 546-conjugated goat anti-mouse IgG1 Ab, Alexa Fluor 633-conjugated goat anti-mouse IgG2b Ab and Alexa Fluor 488-conjugated donkey anti-goat IgG Ab (all from Thermo Fisher Scientific). For detection of T cells, the sections were incubated with Alexa Fluor 647-conjugated rat anti-human CD3 (CD3-12: Bio-Rad, Hercules, CA). After being stained, sections were mounted with ProLong Gold with DAPI (Thermo Fisher Scientific) and examined with a Leica TCS SPE confocal microscope (Leica Microsystems, Heerbrugg, Switzerland).

To stain IL-10$^+$ ILCs in mouse lungs, lung tissues from saline-treated and HDM-treated

IL-10^{venus} mice were embedded in OCT compound (Sakura Finetek) and stored at -80°C until use. 6-μm-thick sections were placed on glass slides and then fixed in ice-cold acetone and methanol (1:1) for 1 min. After three washes in PBS, the sections were blocked with 10% (vol/vol) goat serum (Nichirei, Tokyo, Japan) for 30 min and incubated with rat anti-mouse sca-1 Ab (D7, BioLegend), hamster anti-mouse CD3 Ab (500A2, BD Biosciences) and rabbit anti-GFP/venus Ab (Medical & Biological Laboratories, Nagoya, Japan) overnight at 4°C. After three washes in PBS, the sections were incubated with secondary Abs such as Alexa Fluor 546-conjugated goat anti-rat IgG Ab, Alexa Fluor 647-conjugated goat anti-hamster IgG Ab and Alexa Fluor 488-conjugated goat anti-rabbit IgG Ab for 1 h at room temperature. After staining, the sections were mounted with ProLong Diamond Antifade Mountant with DAPI (Thermo Fisher Scientific) and examined with a confocal microscope (LSM 510 META ConfoCor, 3, Carl Zeiss, Oberkochen, Germany).

To stain RALDH-1 in mouse lungs, lungs from saline-treated and HDM-treated mice were fixed with 4% PFA for 24 h and embedded in paraffin. 5-μm-thick sections were deparaffinized, followed by antigen retrieval (Target Retrieval Solution, Agilent). After three washes in PBS, the sections were blocked with 1.5 % (wt/vol) horse serum for 20 min and then incubated with rabbit anti-mouse ALDH1A1 Ab (EP1933Y, Abcam) or isotype Ab overnight at 4°C. After three washes in PBS, the Envision G/2 System/AP (Agilent) was used according to the manufacturer's instructions, followed by counterstaining with hematoxylin.

RNA isolation and sequencing analysis of RNA-seq data

Total RNA was prepared from sorted $CD45^{+}Lin^{-}CD161^{+}IL\text{-}10^{+}$ cells and

111 $CD45^{+}Lin^{-}CD161^{+}IL\text{-}10^{-}$ cells using the RNeasy Plus micro Kit (QIAGEN). The quantity
112 and quality of the isolated RNA were determined with a Qubit® (1.0) Fluorometer (Life
113 Technologies, CA) and a Bioanalyzer 2100 (Agilent) and samples with an RNA integrity
114 number of >7.0 were chosen for sequencing. Library preparation for RNA-seq was
115 performed using the TruSeq Stranded mRNA Sample Prep Kit (Illumina, CA).
116 Total RNA samples (1 μg) were ribosome-depleted and then reverse-transcribed into
117 double-stranded cDNA with actinomycin added during first-strand synthesis. The cDNA
118 samples were fragmented, end-repaired and polyadenylated before ligation with TruSeq
119 adapters. The adapters contain the index for multiplexing. Fragments containing TruSeq
120 adapters on both ends were selectively enriched by PCR. The quality and quantity of the
121 enriched libraries were validated using a Qubit® (1.0) Fluorometer and Bioanalyzer 2100
122 (Agilent). The product was a smear with an average fragment size of approximately 360 bp.
123 The libraries were normalized to 10nM in 10 mM Tris-Cl, pH8.5 with 0.1% Tween 20.
124 A TruSeq SR Cluster Kit v4-cBot-HS or TruSeq PE Cluster Kit v4-cBot-HS (Illumina) was
125 used for cluster generation using 8 pM of pooled normalized libraries on the cBOT.
126 Sequencing was performed on an Illumina HiSeq 2500 paired end at 2x126 bp or single end
127 126 bp using a TruSeq SBS Kit v4-HS (Illumina). Raw data is available at GEO with
128 accession number: GSE110278.
129 Sequencing images were transformed with Illumina Basecaller software to bcl files, which
130 were demultiplexed to FASTQ files with CASAVA v1.8.2 software (Illumina). Quality check
131 on the reads was performed with FASTQ (v.0.10.0, Babraham Institute, Cambridge, UK).
132 Raw sequencing reads were mapped to the *Homo sapiens* genome (version GRCh37) using

RSEM (v1.2.12)[1] implementation of Bowtie software (v 1.0.0)[2] alignment program with the Ensembl annotation (v 75). Gene and isoform level abundances were quantified as RPKM values. All analyses were performed using the R statistical software (version 3.2.0; R Foundation for Statistical Computing, Vienna, Austria). Clustering analyses were performed using the "ward.D2" clustering algorithm implemented in the "hclust" function of R statistics package. Heatmap plots were prepared with the function "heatmap.2" implemented in the gplots R package.

Differential expression analysis between two groups was performed using the edgeR bioconductor package.[3] Genes present in less than 75% of samples in both conditions were removed. Q-values were calculated using the Benjamini-Hochberg method and genes with a q-value <0.05 and an absolute value of log2 (fold change)>1 were kept for further analysis. Gene ontology (GO) term enrichment analysis was performed using the GOseq bioconductor package[4] using the Wallenius approximation.

Human nasal tissues

Harvesting human nasal tissue from healthy controls and patients with CRS have been performed according to the Helsinki declarations and Swiss law. The study on nasal mucosal immunology was approved by the ethical committee of Zurich (KEK ZH 2011-514 and its amendment in 2012). All subjects included in the study gave written informed consent.

Tissue from control patients was harvested during standard septoplasty procedures from the inferior turbinate, when performing an anterior turbinoplasty. Polyp tissue was obtained during standard FESS procedures.

155

156 **Cell isolation from human tissues**

157 Nasal tissues were cut into fine pieces and then digested for 45 min at 37°C in RPMI medium
158 (Thermo Fisher Scientific) with 2mg/ml collagenase type II (Worthington, Lakewood, NJ)
159 and 0.04 μg/ml DNase I (Roche, Basel, Switzerland). After incubation, cells were
160 dissociated using GentleMACS Dissociator (Miltenyi Biotec). Lung tissues were collected
161 from tumor patients undergoing lobectomy. A small piece of normal lung tissue was cut out
162 from a part distal from the tumor-affected region. The tissue was minced, washed with PBS
163 and filtered with a 100-μm filter. Subsequently, tissues were digested for 40 min at 37°C in
164 RPMI medium (Thermo Fisher Scientific) with 0.25 mg/ml collagenase type II
165 (Sigma-Aldrich) and 0.2 mg/ml DNase (Roche). After incubation, cold RPMI medium
166 (0.25ml of 200mM L-glutamine, 1% penicillin/streptomycin) was added to stop the
167 digestion, and the tissues were mechanically disrupted using a 50-ml syringe and 100-μm
168 filter. Cell debris and larger alveolar macrophages were separated by density centrifugation
169 using 30% Percoll (GE Healthcare, Chalfont, UK).

170

171 **Cell cultures of human bronchial epithelial cells**

172 Primary bronchial epithelial cells from healthy individuals were expanded as monolayers in
173 bronchial epithelial cell basal medium supplemented with the SingleQuots Kit (Lonza, Basel,
174 Switzerland) and then seeded at a density of 150,000 cells in a 6.5-mm diameter polyester
175 membrane with a pore size of 0.4 μm. Cells were cultured in the medium for ALI culture
176 described elsewhere[5] until their growth reached complete confluence. Subsequently, the

177 medium in the apical compartment was removed to allow the cells to differentiate. Cells were
178 used in experiments when the transepithelial electric resistance (TER) reached a plateau.
179
180
181 **House dust mite (HDM)-induced allergic airway inflammation**
182 Mice were treated intranasally with 20 μl of 1.25 mg/ml HDM extract (Greer Laboratories,
183 Lenoir, NC) in saline or saline alone, 5 days per week for three consecutive weeks. Three
184 days after the last intranasal administration, the mice were sacrificed and analyzed.
185
186 **Bronchoalveolar lavage fluid (BALF)**
187 Mice were intubated with a 22-G blunt needle (NIPRO, Osaka, Japan) and 1 ml of HBSS
188 containing 2% FCS was injected through the needle into the lungs. The number of each cell
189 type was counted with an automated hematology analyzer, Sysmex XT-1800i (Sysmec
190 Corporation, Hyogo, Japan). ILC2s in the BALFs were analyzed by flow cytometry.
191
192 **Isolation of mouse ILC2s from the mesentery**
193 ILC2s were isolated from the mesentery as described described by others.[7] In brief, mice
194 underwent transcardial perfusion with PBS to eliminate blood leukocytes, and then the
195 mesentery was dissected from the intestine. The mesentery was minced with scissors and
196 incubated at 37°C for 60 min in DMEM containing 4% BSA (Sigma-Aldrich), 20 μg/ml
197 Liberase DH (Roche) and 1 μg/ml DNase I (Roche). Lin^- $CD127^+$ $sca\text{-}1^+$ $KLRG\text{-}1^+$ ILC2s
198 were determined by flow cytometry.

Fig E1. RNA sequencing of IL-10$^+$ and IL-10$^-$ ILCs

A, Gating strategy to sort IL-10$^+$ and IL-10$^-$ ILCs using an IL-10 secretion assay. **B,** Hierarchical clustering of gene expression. **C,** Flow cytometric analyses of IL-10$^+$ and ILC2s. **D,** Gene expression profiles of IL-10$^+$ and IL-10$^-$ ILCs.

Fig E2. Suppression assay

A, Division of CFSE-labeled CD4$^+$ T cells in the presence of IL-10$^-$ ILCs at different ratios. **B,** Division of CFSE-labeled ILC2s in the presence of IL-10$^-$ ILCs at different ratios. **C,** Division of CFSE-labeled ILC2s in the presence of Treg cells at different ratios. The CFSE fluorescence level was analyzed by flow cytometry, and the division index was calculated. Data are shown as the mean ± SEM. n = 3 per group, in duplicate. *P<0.05, **P<0.01 between indicated groups.

Fig E3. Stability of IL-10$^+$ and IL10$^-$ ILCs

The experimental protocol and the data are shown. Human ILC2 cell lines were stimulated for 3 days with IL-2, IL-33 and RA, and IL-10$^+$ and IL-10$^-$ cells were sorted using an IL-10 secretion assay. The sorted IL-10$^+$ and IL-10$^-$ ILCs were then cultured for 3 days in the presence of IL-2. Subsequently, half of the cells were stimulated for 5 hours with PMA plus Ionomycin in the presence of Brefeldin A for final 3 hours. The other half of the cells were restimulated with IL-2, IL-33 and RA for 3days, followed by stimulation with PMA, Ionomycin and Brefeldin A. The frequencies of IL-10$^+$ cells were determined by flow

cytometry (n = 4)

FIG E4. A fraction of ILC2 clones give rise to IL-10-producing ILCregs in response to RA.

ILC2 clones were expanded with irradiated PBMCs and recombinant human IL-2 for 3 weeks. A, ILC2 clones were stimulated with IL-2, or IL-2, IL-33 and all-trans RA, for 3 days. The frequency of IL-10^+ ILCs in each ILC2 clones was determined by flow cytometry. B, The levels of IL-10 in culture supernatants of ILC2 clones stimulated with IL-2, IL-33 and all-trans RA were determined by ELISA. C, The expression levels of c-Kit, CD161, CTLA-4 and IL-13 before all-trans RA stimulation were determined by flow cytometry. Blue dots (left: n = 25) represent clones that remained IL-10-negative after all-trans RA stimulation. Red dots (right: n = 10) represent clones that started to produce IL-10 after all-trans RA stimulation. D, The levels of IL-5 and IL-13 in culture supernatants of ILC2 clones stimulated with IL-2, IL-33 and all-trans RA were determined by ELISA.
Blue dots (left: n = 25) represent clones that remained IL-10-negative after all-trans RA stimulation. Red dots (right: n = 10) represent clones that started to produce IL-10 after all-trans RA stimulation. Data are shown as the mean ± SEM. NS: not significant between indicated groups.

FIG E5. Frequency of IL-10^+ immune cells in an HDM-induced asthma-like model

A, Gating strategy for identifying IL-10-producing $CD4^+$ T cells, $CD19^+$ B cells and ILCs in lungs from saline- or HDM-treated mice. **B,** Frequency of IL-10^+ immune cells in lungs from

mice 72 h after the last intranasal inhalation (saline, n = 8; and HDM, n = 16).

1. Li B, Dewey CN. RSEM: accurate transcript quantification from RNA-Seq data with or without a reference genome. BMC Bioinformatics 2011; 12:323.
2. Langmead B, Trapnell C, Pop M, Salzberg SL. Ultrafast and memory-efficient alignment of short DNA sequences to the human genome. Genome Biol 2009; 10:R25.
3. Robinson MD, McCarthy DJ, Smyth GK. edgeR: a Bioconductor package for differential expression analysis of digital gene expression data. Bioinformatics 2010; 26:139-40.
4. Young MD, Wakefield MJ, Smyth GK, Oshlack A. Gene ontology analysis for RNA-seq: accounting for selection bias. Genome Biol 2010; 11:R14.
5. Kubo T, Wawrzyniak P, Morita H, Sugita K, Wanke K, Kast JI, et al. CpG-DNA enhances the tight junction integrity of the bronchial epithelial cell barrier. J Allergy Clin Immunol 2015; 136:1413-6 e1-8.
6. Atarashi K, Tanoue T, Shima T, Imaoka A, Kuwahara T, Momose Y, et al. Induction of colonic regulatory T cells by indigenous Clostridium species. Science 2011; 331:337-41.
7. Moro K, Ealey KN, Kabata H, Koyasu S. Isolation and analysis of group 2 innate lymphoid cells in mice. Nat Protoc 2015; 10:792-806.